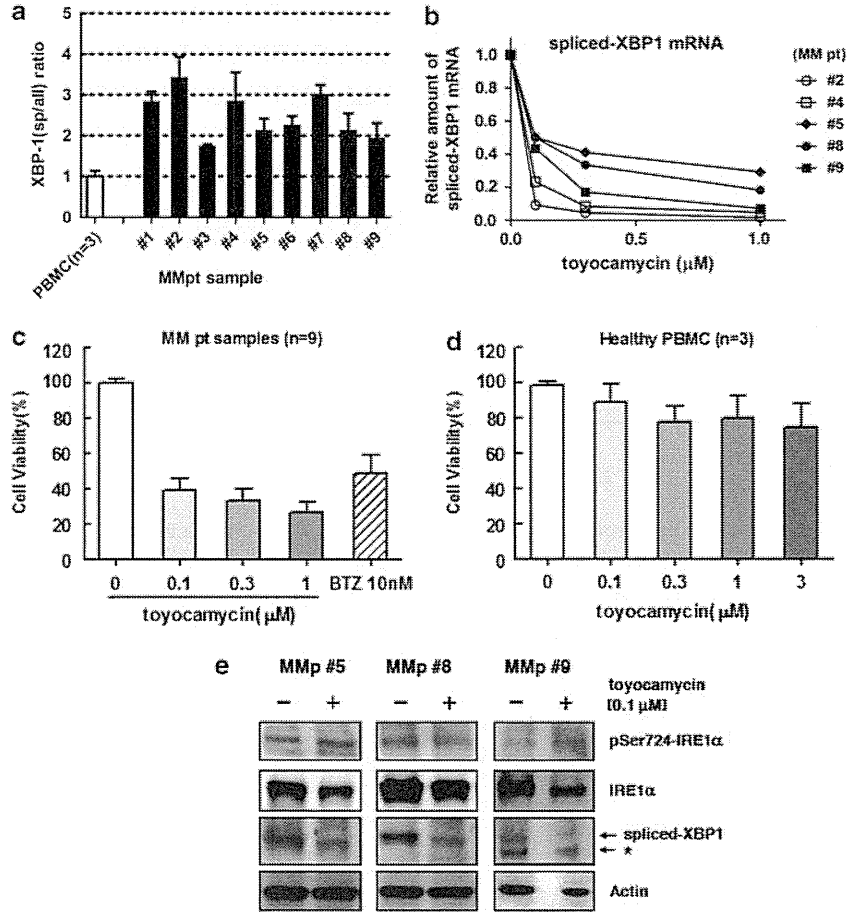

Figure 5. Sensitivity of primary MM cells to toyocamycin treatment. (**a**) The ratio of the spliced form of XBP1 to all forms (spliced and non-spliced) in nine primary MM cells and three healthy donors' PBMC. To compare the ratios among the 12 samples, the ratio in healthy PBMC was defined as the control. Each column represents the mean + s.d. of three independent experiments. (**b**) Altered amount of spliced-XBP1 mRNA after exposure to toyocamycin for 6 h at the indicated concentrations. The amount was quantitated by real-time PCR method. Data represent the mean of three independent experiments. (**c**) Analysis of cellular viability of primary MM cells ($n = 9$) after exposure to toyocamycin or BTZ for 24 h at the indicated concentrations. The primary MM cells derived from eight patients were evaluated with mean + s.d. being plotted. (**d**) Analysis of cellular viability of PBMC ($n = 3$) derived from healthy donors after exposure to toyocamycin for 24 h at the indicated concentrations. Each column represents the mean + s.d. of three independent experiments. (**e**) Altered expression levels of IRE1-XBP1 pathway-related molecules in primary MM cells on exposure to toyocamycin. The primary MM cells (#5, #8 and #9) were cultured in the presence of 0.1 μM toyocamycin for 6 h. Expression levels of spliced forms of XBP1, IRE1 and pSer724-phosphorylated IRE1 were evaluated by immunoblot analysis. *Depicts non-specific band.

activities, such as PKC,[45] cdc2[46] or PI4K.[47] Considering the structure of toyocamycin and its analogs, it was also predicted that it would inhibit IRE1 auto-phosphorylation. However, it inhibited IRE1 phosphorylation on Ser724 not only in IRE1-overexpressing 293T cells (Figure 2c) but also in MM cell lines (Figures 3c and 5e). Recent studies have suggested that the trigger for IRE1 endoribonuclease activity is not phosphorylation but a conformational change in the kinase domain induced by cofactor (ATP or ADP) binding. Therefore, it is likely that toyocamycin inhibits IRE1α-induced XBP1 mRNA cleavage through a cofactor-induced conformational change of IRE1α rather than inhibition of IRE1α auto-phosphorylation.

Previous studies have suggested that the IRE1α-XBP1 pathway has a critical role in ER stress-induced cytoprotection. 1NM-PP1, a small molecule selectively activating the IRE1α(I642G) mutant,[18] protected cells from tunicamycin- or thapsigargin-induced cell death.[48,49] In contrast, overexpression of dominant-negative XBP1 or knockdown of XBP1 has been reported to enhance tunicamycin-induced apoptosis.[50] Consistent with previous reports, we also found that toyocamycin synergistically induced cell death in ER-stressed HeLa, HT29 and HCT116 cells (Supplementary Figure 2 and data not shown). More recently, as with toyocamycin, STF-083010 was shown to inhibit IRE1 ndonuclease activity without affecting its kinase activity *in vitro*.[14] However, these compounds mediate their inhibitory activity at ⩾60 μM, and show little MM cell apoptosis induction as single agents. STF-083010 also shows anti-tumor activity in human MM xenograft models. However, while toyocamycin suppressed tumor volume to around 50% at 1 mg/kg by once-weekly injection, the STF-083010 dose needed to be 30 mg/kg by once-weekly injection.[14] In our study, adenosine analogs showed potent inhibition of ER stress-induced IRE1α-XBP1 activation at the nanomolar level. Compared with these, toyocamycin induced marked apoptosis in ER-stressed tumor cells and MM cells at much lower concentrations. In addition, it also inhibited the constitutive activation of XBP1 in MM cells even at suboptimal concentrations such as 10 nM. However, the mechanism by which toyocamycin mediates dose-dependent apoptosis remains unknown. Although three MM cell lines with low active XBP1 expression showed lower sensitivity to toyocamycin treatment than other seven MM cells

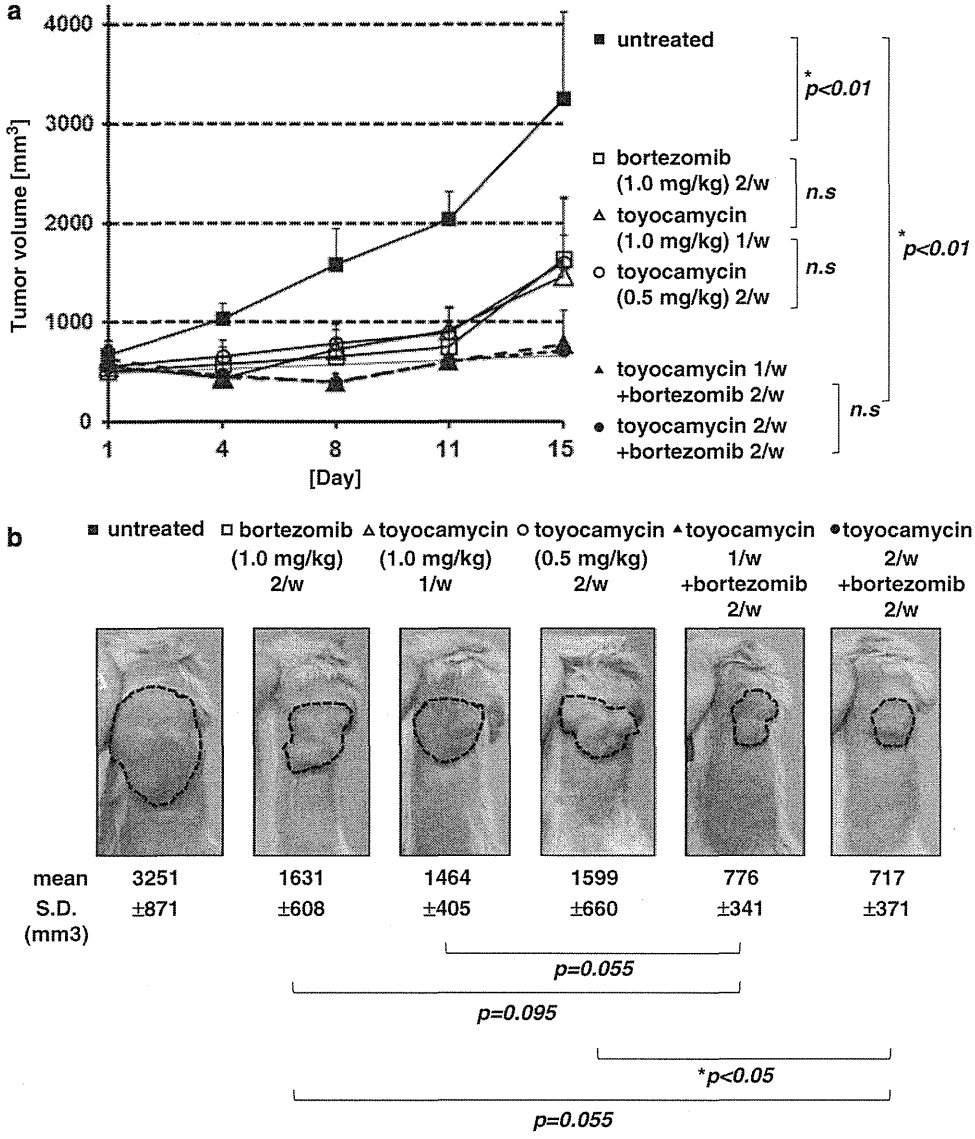

Figure 6. Toyocamycin exerts anti-tumor activity in an *in vivo* MM model. (**a**) Average tumor volume in untreated mice (5% Traubenzucker alone) and mice treated with bortezomib alone, toyocamycin alone or with combination of bortezomib and toyocamycin at the indicated dose. (**b**) Representative images and mean values of tumor size observed at day 15 in each group; closed square, untreated; open square, bortezomib-treated (1.0 mg/kg) twice a week; open triangle, toyocamycin-treated (1.0 mg/kg) once a week; open circle, toyocamycin-treated (0.5 mg/kg) twice a week; closed triangle, toyocamycin (1.0 mg/kg, once a week) + bortezomib (1.0 mg/kg, twice a week)-treated; and closed circle, toyocamycin (0.5 mg/kg, twice a week) + bortezomib (1.0 mg/kg, twice a week)-treated. *Represents statistically significant.

with high active XBP1 expression, these three cell lines still demonstrated sensitivity to the drug at the nM concentration. It may be speculated that toyocamycin also triggers another stress-inducing factor at higher concentrations, which may induce strong apoptosis under IRE1α-XBP1-suppressed conditions. Further analysis needs be conducted to elucidate the whole picture of its mechanisms of action on MM cells.

An earlier phase I toyocamycin single-agent study also testing possible anti-tumor effects in patients with advanced solid tumors has been reported.[51] However, because no apparent clinical responses were observed in that study, further clinical evaluation was not planned. In that study, toyocamycin showed no systemic side effects, such as organ dysfunction and cytopenia, and only local necrosis at the site of infusion was reported to occur when the drug was delivered into the soft tissues. This suggests that toyocamycin adverse events could be manageable if it is infused through central venous catheters. In addition, this study does not exclude potential clinical efficacy of toyocamycin against solid tumors, because it was a phase I trial lacking evaluation of stable disease often applied in more recent clinical trials of molecular-targeting therapies.

In conclusion, we demonstrated that the adenosine analog toyocamycin has a potent IRE1-XBP1 inhibitory effect on ER-stressed tumors and MM cells, as well as triggering dose-dependent apoptosis in these cells. These results provide a preclinical rationale for clinical trials of toyocamycin and other adenosine analogs alone and in combination with BTZ for treating MM.

CONFLICT OF INTEREST

Y Shiotsu is an employee of Kyowa Hakko Kirin Co., Ltd, Japan. S Iida received research funding from Kyowa Hakko Kirin and Chugai Pharmaceutical Co., Ltd.

S Iida declares honoraria from Janssen Pharmaceutical KK. The other authors declare no conflict of interest.

ACKNOWLEDGEMENTS

We thank Dr Masayuki Igarashi, Dr Masaki Hatano, Mrs Naoko Kinoshita and Dr Yoshio Nishimura (Institute of Microbial Chemistry, Tokyo, Japan) for fermentation of *Actinomycete* strain MK653-101F13, and Ms Chiori Fukuyama (Nagoya City University) for her skillful technical assistance. This study was partly supported by grants from Takeda Science Foundation. This work was partly supported by a Grant-in-Aid for Scientific Research from the Ministry of Education, Culture, Sports, Science and Technology (23791805) and a Grant-in-Aid for Cancer Research from the Ministry of Health, Labor and Welfare (21-8-5), Japan.

REFERENCES

1 Kumar S, Rajkumar SV. Many facets of bortezomib resistance/susceptibility. *Blood* 2008; **112**: 2177–2178.
2 Shah JJ, Orlowski RZ. Proteasome inhibitors in the treatment of multiple myeloma. *Leukemia* 2009; **23**: 1964–1979.
3 Reimold AM, Iwakoshi NN, Manis J, Vallabhajosyula P, Szomolanyi-Tsuda E, Gravallese EM *et al.* Plasma cell differentiation requires the transcription factor XBP-1. *Nature* 2001; **412**: 300–307.
4 Shaffer AL, Lin KI, Kuo TC, Yu X, Hurt EM, Rosenwald A *et al.* Blimp-1 orchestrates plasma cell differentiation by extinguishing the mature B cell gene expression program. *Immunity* 2002; **17**: 51–62.
5 Munshi NC, Hideshima T, Carrasco D, Shammas M, Auclair D, Davies F *et al.* Identification of genes modulated in multiple myeloma using genetically identical twin samples. *Blood* 2004; **103**: 1799–1806.
6 Carrasco DR, Sukhdeo K, Protopopova M, Sinha R, Enos M, Carrasco DE *et al.* The differentiation and stress response factor XBP-1 drives multiple myeloma pathogenesis. *Cancer Cell* 2007; **11**: 349–360.
7 Shuda M, Kondoh N, Imazeki N, Tanaka K, Okada T, Mori K *et al.* Activation of the ATF6, XBP1 and grp78 genes in human hepatocellular carcinoma: a possible involvement of the ER stress pathway in hepatocarcinogenesis. *J Hepatol* 2003; **38**: 605–614.
8 Lee K, Tirasophon W, Shen X, Michalak M, Prywes R, Okada T *et al.* IRE1-mediated unconventional mRNA splicing and S2P-mediated ATF6 cleavage merge to regulate XBP1 in signaling the unfolded protein response. *Genes Dev* 2002; **16**: 452–466.
9 Asosingh K, De Raeve H, de Ridder M, Storme GA, Willems A, Van Riet I *et al.* Role of the hypoxic bone marrow microenvironment in 5T2MM murine myeloma tumor progression. *Haematologica* 2005; **90**: 810–817.
10 Martin SK, Diamond P, Gronthos S, Peet DJ, Zannettino AC. The emerging role of hypoxia, HIF-1 and HIF-2 in multiple myeloma. *Leukemia* 2011; **25**: 1533–1542.
11 Smith KD, Wrenshall LE, Nicosia RF, Pichler R, Marsh CL, Alpers CE *et al.* Delayed graft function and cast nephropathy associated with tacrolimus plus rapamycin use. *J Am Soc Nephrol* 2003; **14**: 1037–1045.
12 Bagratuni T, Wu P, Gonzalez de Castro D, Davenport EL, Dickens NJ, Walker BA *et al.* XBP1s levels are implicated in the biology and outcome of myeloma mediating different clinical outcomes to thalidomide-based treatments. *Blood* 2010; **116**: 250–253.
13 Bae J, Carrasco R, Lee AH, Prabhala R, Tai YT, Anderson KC *et al.* Identification of novel myeloma-specific XBP1 peptides able to generate cytotoxic T lymphocytes: a potential therapeutic application in multiple myeloma. *Leukemia* 2011; **25**: 1610–1619.
14 Papandreou I, Denko NC, Olson M, Van Melckebeke H, Lust S, Tam A *et al.* Identification of an Ire1alpha endonuclease specific inhibitor with cytotoxic activity against human multiple myeloma. *Blood* 2011; **117**: 1311–1314.
15 Bertolotti A, Zhang Y, Hendershot LM, Harding HP, Ron D. Dynamic interaction of BiP and ER stress transducers in the unfolded-protein response. *Nat Cell Biol* 2000; **2**: 326–332.
16 Korennykh AV, Egea PF, Korostelev AA, Finer-Moore J, Zhang C, Shokat KM *et al.* The unfolded protein response signals through high-order assembly of Ire1. *Nature* 2009; **457**: 687–693.
17 Shamu CE, Walter P. Oligomerization and phosphorylation of the Ire1p kinase during intracellular signaling from the endoplasmic reticulum to the nucleus. *EMBO J* 1996; **15**: 3028–3039.
18 Papa FR, Zhang C, Shokat K, Walter P. Bypassing a kinase activity with an ATP-competitive drug. *Science* 2003; **302**: 1533–1537.
19 Aragon T, van Anken E, Pincus D, Serafimova IM, Korennykh AV, Rubio CA *et al.* Messenger RNA targeting to endoplasmic reticulum stress signalling sites. *Nature* 2009; **457**: 736–740.
20 Sidrauski C, Walter P. The transmembrane kinase Ire1p is a site-specific endonuclease that initiates mRNA splicing in the unfolded protein response. *Cell* 1997; **90**: 1031–1039.
21 Lee KP, Dey M, Neculai D, Cao C, Dever TE, Sicheri F. Structure of the dual enzyme Ire1 reveals the basis for catalysis and regulation in nonconventional RNA splicing. *Cell* 2008; **132**: 89–100.
22 Shen X, Ellis RE, Lee K, Liu CY, Yang K, Solomon A *et al.* Complementary signaling pathways regulate the unfolded protein response and are required for C. elegans development. *Cell* 2001; **107**: 893–903.
23 Yoshida H, Matsui T, Yamamoto A, Okada T, Mori K. XBP1 mRNA is induced by ATF6 and spliced by IRE1 in response to ER stress to produce a highly active transcription factor. *Cell* 2001; **107**: 881–891.
24 Tashiro E, Hironiwa N, Kitagawa M, Futamura Y, Suzuki S, Nishio M *et al.* Trierixin, a novel Inhibitor of ER stress-induced XBP1 activation from Streptomyces sp. 1. Taxonomy, fermentation, isolation and biological activities. *J Antibiot* 2007; **60**: 547–553.
25 Nishimura H, Katagiri K, Sato K, Mayama M, Shimaoka N. Toyocamycin, a new anti-candida antibiotics. *J Antibiot* 1956; **9**: 60–62.
26 Ri M, Iida S, Nakashima T, Miyazaki H, Mori F, Ito A *et al.* Bortezomib-resistant myeloma cell lines: a role for mutated PSMB5 in preventing the accumulation of unfolded proteins and fatal ER stress. *Leukemia* 2010; **24**: 1506–1512.
27 Tashiro E, Maruki H, Minato Y, Doki Y, Weinstein IB, Imoto M. Overexpression of cyclin D1 contributes to malignancy by up-regulation of fibroblast growth factor receptor 1 via the pRB/E2F pathway. *Cancer Res* 2003; **63**: 424–431.
28 Iwawaki T, Akai R. Analysis of the XBP1 splicing mechanism using endoplasmic reticulum stress-indicators. *Biochem Biophys Res Commun* 2006; **350**: 709–715.
29 Yano H, Kayukawa S, Iida S, Nakagawa C, Oguri T, Sanda T *et al.* Overexpression of carboxylesterase-2 results in enhanced efficacy of topoisomerase I inhibitor, irinotecan (CPT-11), for multiple myeloma. *Cancer Sci* 2008; **99**: 2309–2314.
30 Kawamura T, Tashiro E, Yamamoto K, Shindo K, Imoto M. SAR study of a novel triene-ansamycin group compound, quinotrierixin, and related compounds, as inhibitors of ER stress-induced XBP1 activation. *J Antibiot* 2008; **61**: 303–311.
31 Suhadolnik RJ, Uematsu T, Uematsu H. Toyocamycin: phosphorylation and incorporation into RNA and DNA and the biochemical properties of the triphosphate. *Biochim Biophys Acta* 1967; **149**: 41–49.
32 Tavitian A, Uretsky SC, Acs G. The effect of toyocamycin on cellular RNA synthesis. *Biochim Biophys Acta* 1969; **179**: 50–57.
33 Yoshida H, Matsui T, Hosokawa N, Kaufman RJ, Nagata K, Mori K. A time-dependent phase shift in the mammalian unfolded protein response. *Dev Cell* 2003; **4**: 265–271.
34 Lee AH, Iwakoshi NN, Glimcher LH. XBP-1 regulates a subset of endoplasmic reticulum resident chaperone genes in the unfolded protein response. *Mol Cell Biol* 2003; **23**: 7448–7459.
35 Haze K, Yoshida H, Yanagi H, Yura T, Mori K. Mammalian transcription factor ATF6 is synthesized as a transmembrane protein and activated by proteolysis in response to endoplasmic reticulum stress. *Mol Biol Cell* 1999; **10**: 3787–3799.
36 Ye J, Rawson RB, Komuro R, Chen X, Dave UP, Prywes R *et al.* ER stress induces cleavage of membrane-bound ATF6 by the same proteases that process SREBPs. *Mol Cell* 2000; **6**: 1355–1364.
37 Shen J, Chen X, Hendershot L, Prywes RER. stress regulation of ATF6 localization by dissociation of BiP/GRP78 binding and unmasking of Golgi localization signals. *Dev Cell* 2002; **3**: 99–111.
38 Okada T, Haze K, Nadanaka S, Yoshida H, Seidah NG, Hirano Y *et al.* A serine protease inhibitor prevents endoplasmic reticulum stress-induced cleavage but not transport of the membrane-bound transcription factor ATF6. *J Biol Chem* 2003; **278**: 31024–31032.
39 Nadanaka S, Yoshida H, Kano F, Murata M, Mori K. Activation of mammalian unfolded protein response is compatible with the quality control system operating in the endoplasmic reticulum. *Mol Biol Cell* 2004; **15**: 2537–2548.
40 Harding HP, Novoa I, Zhang Y, Zeng H, Wek R, Schapira M *et al.* Regulated translation initiation controls stress-induced gene expression in mammalian cells. *Mol Cell* 2000; **6**: 1099–1108.
41 Harding HP, Zhang Y, Ron D. Protein translation and folding are coupled by an endoplasmic-reticulum-resident kinase. *Nature* 1999; **397**: 271–274.
42 Tirasophon W, Lee K, Callaghan B, Welihinda A, Kaufman RJ. The endoribonuclease activity of mammalian IRE1 autoregulates its mRNA and is required for the unfolded protein response. *Genes Dev* 2000; **14**: 2725–2736.
43 Zhou J, Liu CY, Back SH, Clark RL, Peisach D, Xu Z *et al.* The crystal structure of human IRE1 luminal domain reveals a conserved dimerization interface required for activation of the unfolded protein response. *Proc Natl Acad Sci USA* 2006; **103**: 14343–14348.

44 Yen L, Svendsen J, Lee JS, Gray JT, Magnier M, Baba T *et al.* Exogenous control of mammalian gene expression through modulation of RNA self-cleavage. *Nature* 2004; **431**: 471–476.

45 Osada H, Sonoda T, Tsunoda K, Isono K. A new biological role of sangivamycin; inhibition of protein kinases. *J Antibiot* 1989; **42**: 102–106.

46 Osada H, Cui CB, Onose R, Hanaoka F. Screening of cell cycle inhibitors from microbial metabolites by a bioassay using a mouse cdc2 mutant cell line, tsFT210. *Bioorg Med Chem* 1997; **5**: 193–203.

47 Nishioka H, Sawa T, Hamada M, Shimura N, Imoto M, Umezawa K. Inhibition of phosphatidylinositol kinase by toyocamycin. *J Antibiot* 1990; **43**: 1586–1589.

48 Lin JH, Li H, Yasumura D, Cohen HR, Zhang C, Panning B *et al.* IRE1 signaling affects cell fate during the unfolded protein response. *Science* 2007; **318**: 944–949.

49 Han D, Upton JP, Hagen A, Callahan J, Oakes SA, Papa FR. A kinase inhibitor activates the IRE1alpha RNase to confer cytoprotection against ER stress. *Biochem Biophys Res Commun* 2008; **365**: 777–783.

50 Lee AH, Iwakoshi NN, Anderson KC, Glimcher LH. Proteasome inhibitors disrupt the unfolded protein response in myeloma cells. *Proc Natl Acad Sci USA* 2003; **100**: 9946–9951.

51 Wilson WL. Phase I study with toyocamycin (NSC-63701). *Cancer Chemother Rep* 1968; **52**: 301–303.

Supplementary Information accompanies the paper on Blood Cancer Journal website (http://www.nature.com/bcj)

Kobayashi et al. BMC Chemical Biology 2012, 12:2
http://www.biomedcentral.com/1472-6769/12/2

BMC Chemical Biology

METHODOLOGY ARTICLE Open Access

Comprehensive predictions of target proteins based on protein-chemical interaction using virtual screening and experimental verifications

Hiroki Kobayashi[1†], Hiroko Harada[1†], Masaomi Nakamura[1], Yushi Futamura[1], Akihiro Ito[2], Minoru Yoshida[2], Shun-ichiro Iemura[3], Kazuo Shin-ya[3], Takayuki Doi[4], Takashi Takahashi[5], Tohru Natsume[3], Masaya Imoto[1] and Yasubumi Sakakibara[1*]

Abstract

Background: Identification of the target proteins of bioactive compounds is critical for elucidating the mode of action; however, target identification has been difficult in general, mostly due to the low sensitivity of detection using affinity chromatography followed by CBB staining and MS/MS analysis.

Results: We applied our protocol of predicting target proteins combining *in silico* screening and experimental verification for incednine, which inhibits the anti-apoptotic function of Bcl-xL by an unknown mechanism. One hundred eighty-two target protein candidates were computationally predicted to bind to incednine by the statistical prediction method, and the predictions were verified by *in vitro* binding of incednine to seven proteins, whose expression can be confirmed in our cell system.
As a result, 40% accuracy of the computational predictions was achieved successfully, and we newly found 3 incednine-binding proteins.

Conclusions: This study revealed that our proposed protocol of predicting target protein combining *in silico* screening and experimental verification is useful, and provides new insight into a strategy for identifying target proteins of small molecules.

Background

To understand complex cell systems, functional analysis of proteins has become the main focus of growing research fields of biology in the post-genome era; however, the roles of many proteins in cellular events remain to be elucidated. Among various methods to elucidate protein functions, the approach of chemical genetics is notable, with small molecular compounds used as probes to elucidate protein functions within signal pathways [1,2]. Indeed, several bioactive compounds have led to breakthroughs in understanding the functional roles of proteins [3-11]; however, one significant hurdle to developing new chemical probes of biological systems is identifying the target proteins of bioactive compounds, discovered using cell-based small-molecule screening.

A variety of methods and technologies for identifying target proteins have been reported [12]. Among them, affinity chromatography is often used for identifying biological targets of multiple small molecules of interest; however, it is usually very difficult to identify compound-targeted protein with low expression because of the low sensitivity of detection using coomassie brilliant blue (CBB) staining and MS/MS analysis. Thus, target identification of small molecules using affinity chromatography is severely limited. To overcome the limitations of affinity chromatography, we propose a new protocol combining *in silico* screening and experimental verification for identification of target proteins.

In our previous work, we developed an *in-silico* screening system, called "COPICAT" (Comprehensive Predictor of Interactions between Chemical compounds And Target proteins), to predict the comprehensive

* Correspondence: yasu@bio.keio.ac.jp
†Equal contributors
[1]Department of Biosciences and Informatics, Faculty of Science and Technology, Keio University, 3-14-1 Hiyoshi, Kohoku-ku, Yokohama 223-8522, Japan
Full list of author information is available at the end of the article

interaction between small molecules and target proteins [13]. If a target protein is input in the system, a list of chemical compounds which are likely to interact with the protein is predicted. In our previous work, several potential ligands for the androgen receptor were predicted by this system, these predictions were experimentally verified, and a novel antagonist was found [14]. On the other hand, if a chemical compound is input in the system, a list of proteins which are likely to interact with the compound is predicted by the system.

Previously, we isolated the natural product incednine from the fermentation broth of *Streptomyces* sp. ML694-90F3, which consists of a novel skeletal structure, enol-ether amide in the 24-membered macrolactam core, with two aminosugars. In addition, it was reported that incednine induced apoptosis in Bcl-xL-overexpressing human small cell lung carcinoma Ms-1 cells when combined with several anti-tumor drugs including adriamycin, camptothecin, cisplatin, inostamycin, taxol, and vinblastine [15]. Because this compound inhibits the anti-apoptotic function of Bcl-2/Bcl-xL without affecting its binding to pro-apoptotic Bcl-2 family proteins, it may target other proteins associated with the Bcl-2/Bcl-xL-regulated apoptotic pathway. To address the mode of action of incednine underlying its interesting function, we first synthesized affinity-tagged incednine which is biologically active (data not shown), and proteins bound to incednine were separated by SDS-PAGE followed by CBB staining, and each protein band was directly identified using liquid chromatography-tandem mass (LC-MS/MS) spectrometry analysis. Fifty-three proteins were identified as listed in Table 1, and some of which, such as eukaryotic initiation factor 4A3(eIF4A3), prolyl 4-hydroxylase, beta subunit (PDI), heat shock protein 70 (HSP70), and protein phosphatase 2A (PP2A) were reported to relate to cancer cell survival[16-19]. Therefore these were knocked down by siRNA or inhibited by a specific inhibitor, and assessed for their ability to modulate Bcl-2/Bcl-xL anti-apoptotic function, as does incednine. However, the candidate proteins tested did not appear to be the target responsible for modulating Bcl-2/Bcl-xL anti-apoptotic function (Additional file 1). Therefore, the target protein of incednine responsible for modulating Bcl-2/Bcl-xL anti-apoptotic function has not yet been determined, and further candidate proteins as targets of incednine are expected to emerge.

In this context, we propose a new protocol combining *in silico* screening and experimental verification for the identification of target proteins. We first predicted the candidate proteins likely binding to the input compound by applying the COPICAT system, and then employed western blotting to detect the binding of predicted proteins to the input compound. This method solves the problem of the low sensitivity of the traditional method (as illustrated in Figure 1).

Results

Computational prediction of target proteins for incednine

We set the chemical compound "incednine" as the binding ligand, and candidate proteins for the targets of incednine were computationally predicted from the KEGG database by using the statistical prediction method for protein-chemical interaction. The training dataset of protein-chemical interactions to construct the SVM-based statistical learning model was collected from the approved DrugCards data in the DrugBank database [20], and 53 interactions with incednine obtained from our previous binding experiments using affinity chromatography (see Table 1 and Methods) because the prediction accuracy was increased when more training samples of protein-chemical interactions were given to the SVM-based statistical learning model. Among 24,245 human proteins in the KEGG repository, 182 proteins were newly predicted as positive, that is, to interact with incednine with high probability greater than the 0.5 threshold (the default threshold value).

Clustering of computationally predicted proteins

The 182 proteins that were computationally predicted to bind to incednine were clustered by the hierarchical clustering method using 199-dimentional feature vector that was used for encoding amino acid sequences to construct the SVM-based statistical learning model (See Methods section for the details). Note that the similarity based on this 199-dimentional feature vector is different from the sequence similarity, and this similarity measure based on the 199-dimentional vector was proven to work well for protein-chemical interaction predictions in our previous work [13]. For example, 5HTT and AR α-1A showed only about 10% sequence similarity although both were reported to interact with the MDMA drug and successfully predicted by our SVM-based statistical learning method. A cutoff threshold on the constructed clustering tree was determined so that the proteins were clustered into 11 clusters and each cluster had a statistically significant number of members. The proteins predicted to bind to incednine are listed in Additional file 2.

Experimental verification

Next, to examine whether incednine can bind to the proteins, an *in vitro* biotinylated incednine pull-down assay using the lysate of Bcl-xL expressing Ms-1 cells was performed. We tested 16 proteins as pilot experiments, which are selected from each cluster by one or two based on antibody availability. Negative candidates that were predicted not to bind to incednine were extracted for experimental verification. These proteins, positive candidates and negative candidates, are listed in Table 2. Among positive candidate proteins, 2 positive candidates PIK3CG and ACACA were found to bind to

Table 1 List of proteins identified to bind to incednine in our previous binding experiments

Protein	Uniprot ID	Kegg ID
poly 4- hydroxylase, beta submit	P07237	5034
N-acylaminoacyl peptide hydrolase	P13798	327
Heat shock protein 70	P08107	3303/3304
Protein Phosphatase A2	P67775	5515
Similar to DNA damage-binding protein 1	Q16531	1642
Deoxyhypusin synthase isoform alpha	P49366	1725
Methionine adenosyltransferse alpha/beta	P31153/Q00266/Q9NZL9	4144/4143/27430
4-alpha-glucanotransferse	P35573	178
Actin alpha 4	O43707	81
Eukaryotic Initiation factor 4A3	P38919	9775
Deoxycytidine kinase	P27707	1633
ATP synthase H+ transporting, mitochondrial F1complex, alpha	P25705	498
prohibitin	P35232	5245
proteasome alpha 7subuit	O14818	5688
proteasome(prosome,macropain) subunit alpha type 8	Q8TAA3	143471
centaurin,beta 2	Q15057	23527
heterogeneous nuclear ribonucleoprotein A/B	Q99729	3182
heterogeneous nuclear ribonucleoprotein K	P61978	3190
heterogeneous nuclear ribonucleoprotein D	Q14103	3184
heterogeneous nuclear ribonucleoprotein A2/B1	P22626	3181
heterogeneous nuclear ribonucleoprotein A1	P09651	3178
heterogeneous nuclear ribonucleoprotein M	P52272	4670
small nuclear ribonucleoprotein polypeptide D2 family	P62316	6633
mitochondrial riblosomal protein L2	Q5T653	51069
mitochondrial riblosomal protein L20	Q9BYC9	55052
mitochondrial riblosomal protein L3	Q6IBT2	11222
mitochondrial riblosomal protein L40	Q9NQ50	64976
mitochondrial riblosomal protein L46	B2RD75	26589
mitochondrial riblosomal protein L49	B2R4G6	740
mitochondrial riblosomal protein L1	A6NG03	65008
mitochondrial riblosomal protein L37	Q9BZE1	51253
small nuclear ribonucleoprotein-assosiated protein B and B'	P14678	6628
cAMP-dependent protein kinase, regulatory subunit alpha 1	P10644	5573
phosphoribosyl pyrophosphate synthetase-associated protein 1	B2R6M4	5635
peptidylprolyl isomerase-like 2	Q13356	23759
thymoprotein isoform beta, gamma	P42167	7112
fructose-bisphosphate aldolase A	P04075	226
brain creatine kinase	P12277	1152
enolase 1	P06733	2023
Ewing sarcoma breakpoint region 1	Q5THL0	2130
fusion(involved in t(12;16) in malignant liposarcoma)	Q6IBQ5	2521
GDP dissociation inhibitor 2	Q5SX88	2665
nucleosome assembly protein 1-like 1	P55209	4673
nucleosome assembly protein 1-like 4	Q99733	4676

Table 1 List of proteins identified to bind to incednine in our previous binding experiments *(Continued)*

phosphoglycerate dehydrogenase	O43175	26227
triosephosphate isomerase 1	P60174	7167
clathrin heavy chain 1	Q00610	1213
clathrin heavy poly peptide -like 1	P53675	8218
glutamyl-prolyl tRNA synthetase	P07814	2058
retinoblastoma binding protein 7	Q16576	5931
retinoblastoma binding protein 4	Q09028	5928
tripartite motif-containing 28 protein	Q13263	10155
high glucose-regulated protein 8	Q9Y5A9	51441

incednine, and 5 positive candidates DAPK1, PIK3C2B, PIP5K3, CHD4, GTF2IRD2 did not bind to incednine. Among negative candidate proteins, 2 negative candidates BECN1 and KIF5B did not bind to incednine, and 1 negative candidate PARP1 did bind to incednine (Figure 2). On the other hand, ITPR1, PARP14, PLCB1, KIF1A, KIF21B, and RGPD5, listed as positive candidates in Table 2, were not well expressed and were not detected in Bcl-xL-expressing Ms-1 cells; therefore, accuracy of 40% (4/10), sensitivity of 66.7% (2/3) and precision of 28.6% (2/7) were achieved.

Discussion

For target identification using affinity chromatography, conventional method requires multiple steps as follows; SDS-PAGE, CBB staining, excision of gel, destaining, reduction, trypsinization, and application to LC-MS/MS system (7 steps); these steps can be cumbersome, time-consuming and require expensive installation. Furthermore, CBB staining used in conventional method can detect proteins over nanogram order. In contrast, our proposed protocol for predicting target protein allows us to use western blotting to detect proteins in picogram order. Indeed, we found two incednine-binding proteins by this prediction. Additionally, we can enhance the precision of COPICAT by feeding back the experimental results to the system.

In this work, PIK3CG, PARP1, and ACACA were revealed to bind to incednine by applying our protocol to identify potential target proteins of chemical compounds. These proteins are potential targets of incednine because it has been reported that these proteins are related to cancer survival and drug resistance, as follows.

PI3KCG encodes p110 catalytic subunit isoform p110γ and heterodimerizes with regulatory subunit p101, composing class IB PI3K in the PI3K family [21,22]. Although PIK3CG and PIK3C2B are distant homologous

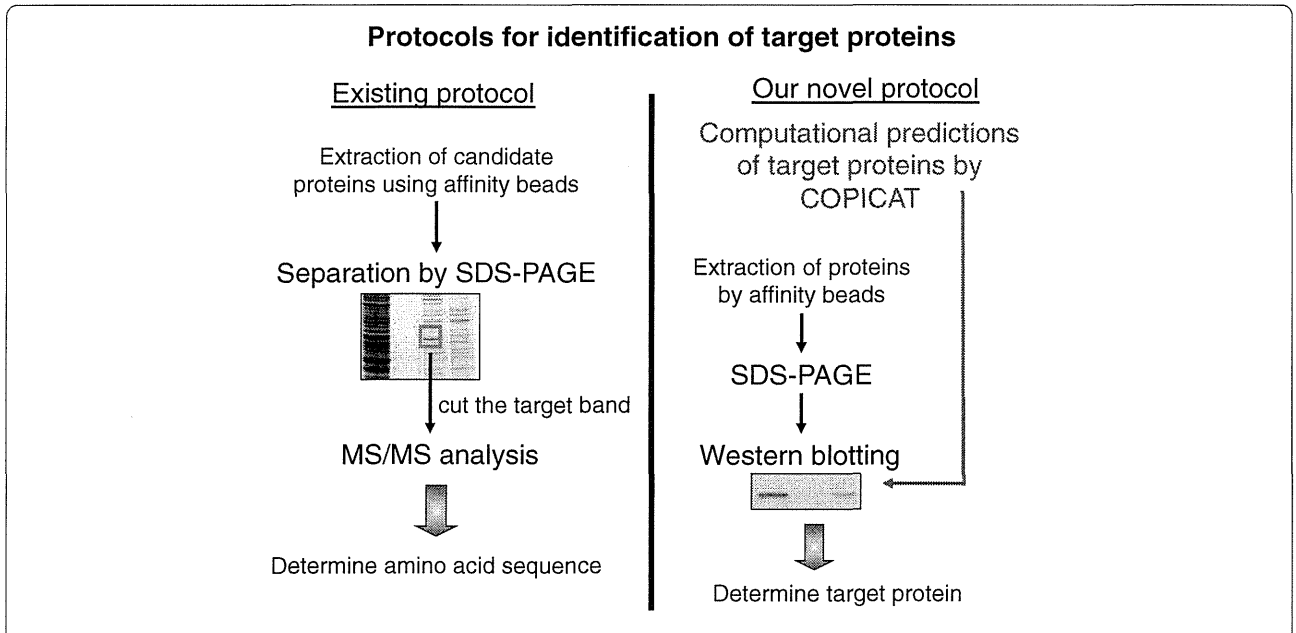

Figure 1 Schematic illustration of our protocol combining *in silico* screening and experimental verification for identification of target protein.

Table 2 Representative proteins selected from each cluster and negative candidates for experimental verification

Cluster No.	Representative Protein
1	ITPR1 (inositol 1,4,5-triphosphate receptor, type 1)
2	DAPK1 (death-associated protein kinase 1)
3	PIK3CG (phosphoinositide-3-kinase, catalytic, gamma polypeptide), PIK3C2B (phosphoinositide-3-kinase, class 2, beta polypeptide)
4	PARP14 (poly (ADP-ribose) polymerase family, member 14)
5	PIP5K3 (phosphatidylinositol-3-phosphate/phosphatidylinositol 5-kinase, type III)
6	PLCB1 (phospholipase C, beta 1)
7	CHD4 (chromodomain helicase DNA binding protein 4)
8	KIF1A (kinesin family member 1A), KIF21B (kinesin family member 21B)
9	ACACA (acetyl-Coenzyme A carboxylase alpha)
10	GTF2IRD2 (GTF2I repeat domain containing 2)
11	RGPD5 (RANBP2-like and GRIP domain-containing protein 5)
Negative	Proteins predicted not to bind to incednine
1	BECN1 (Beclin-1)
2	PARP1 (poly (ADP-ribose) polymerase family, member 1)
3	KIF5B (kinesin family member 5B)

with 20% sequence identity, incednine selectively binds to PIK3CG but not PIK3C2B (Figure 2). In contrast to class IA, class IB PI3K acts downstream of G-protein coupled receptors (GPCR). It has been reported that p110γ was upregulated and activated by the chimeric oncogene Bcr-Abl expression to contribute to cell proliferation and drug resistance in chronic myelogenous leukemia [23], and was found to be highly and specifically expressed among the PI3K family in human pancreatic cancer [24], suggesting that class IB PI3K might relate to cell survival and drug resistance. Product of enzymatic activation of class IB PI3K as class IA, phosphatidylinositol-3,4,5-trisphosphate, makes BAD dissociate from Bcl-xL and promotes cell survival *via* Akt activation [22]. Therefore class IB PI3K might contribute cell survival in Bcl-xL-overexpressing cells.

PARP1 is a member of the PARP protein superfamily that catalyzes the polymerization of ADP-ribose moieties onto target proteins, using NAD^+ as a substrate and releasing nicotine amide in the process [25]. PARP1 activity is important for the regulation of homeostasis and the maintenance of genomic stability, participating in DNA repair, the regulation of transcription, DNA replication, cell differentiation, proliferation and cell death [26-28]. Many *in vitro* and *in vivo* experiments demonstrated that inhibition of PARP1 potentiates the cytotoxicity of anti-cancer drugs and ionizing radiation [29-32]. Therefore, incednine could bind to PARP1 and could function as antagonist of anti-apoptotic PARP1 protein. Alternatively, PARP1 is emerging as an important activator of caspase-independent cell death. It has been previously reported that PARP1 mediates the release of apoptosis-inducing factor (AIF), one of the initiators of

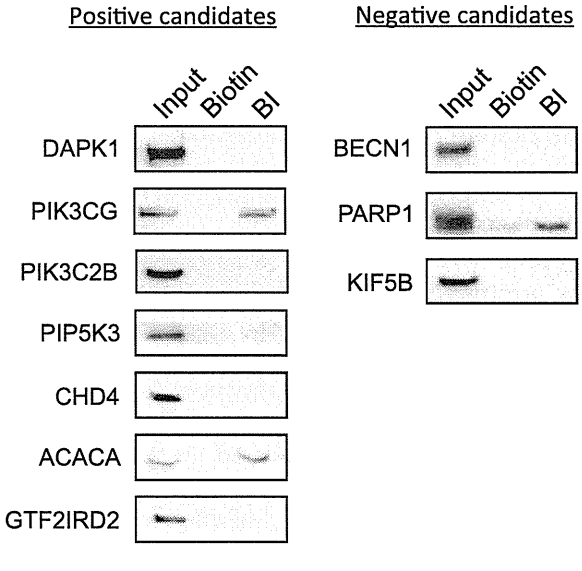

Figure 2 Experimental verification by *in vitro* biotinylated incednine pull-down assay. Lysates from Ms-1 overexpressing Bcl-xL were incubated with biotin (Biotin) or biotinylated incednine (BI) and avidin beads for 3 h. The beads were washed, and co-precipitated proteins were eluted with 2 mM biotin. The eluted proteins were subjected to western blotting using the indicated antibodies. "Positive candidates" means proteins which were predicted to bind to incednine, and "Negative candidates" means proteins which were predicted not to bind to incednine.

caspase-independent cell death, possibly due to enzymatic over-activation [33-35]. We also observed that co-treatment of Bcl-xL-overexpressing Ms-1 cells with incednine and ant-tumor drugs induced AIF release and subsequent caspase-independent cell death (unpublished data); therefore, we can not exclude the possibility that incednine binds to PARP1 and functions as PARP1 agonist by accerelating AIF release.

However, the most likely candidate of an incednine target protein is ACACA (acetyl-CoA carboxylase-α), which was classified in cluster 9. ACACA is the rate-limiting enzyme for long-chain fatty acid synthesis that catalyzes the ATP-dependent carboxylation of acetyl-CoA to malonyl-CoA, playing a critical role in cellular energy storage and lipid synthesis [36]. There is strong evidence that cancer cell proliferation and survival are dependent on *de novo* fatty acid synthesis [37-40]. Additionally, ACACA is upregulated in multiple types of human cancers [41,42]; therefore, ACACA may also contribute to cell survival in Bcl-xL-overexpressing tumor cells. Indeed, our preliminary experiments suggested that chemical inhibition of ACACA using TOFA (5-tetradecyloxy-2-furoic acid, ACACA antagonist) or small interfering RNA-mediated ACACA silencing results in the induction of apoptosis in Bcl-xL-overexpressing human small cell lung carcinoma Ms-1 cells when combined with anti-tumor drugs as does incednine (unpublished observation), suggesting that ACACA might be a molecular target of incednine. The possibility that incednine targets ACACA is being actively investigated.

While our experimental verification implied the relatively low precision value 28.6% (2/7), new detections of two incednine-binding proteins in addition to previously identified 53 proteins are significant. On the other hand, while we selected 7 candidates by clustering 182 predicted proteins for experimental verification, more comprehensive verification experiments for the 182 predicted proteins are needed.

The application of our method to incednine resulted in 28.6% (2/7) precision according to *in vitro* pull-down assay. However, this relatively low precision value does not represent the true statistical significance of the method and is not comparable to the benchmark performances (including 98.4% precision) by 10-fold cross-validation for COPICAT system.

This 28.6% precision can be evaluated by using the following *P*-value.

$$P\text{-}value = \sum_{x=p}^{t} \frac{{}_{M}C_{x} \times {}_{(N-M)}C_{(t-x)}}{{}_{N}C_{t}}$$

Here, N is the number of human proteins, M is the number of proteins potentially binding to the incednine, t is the number of tested proteins, and p is the number of true positives. With N =24,245, which is the number of human proteins in the KEGG repository, and $M = N \times 1\% \fallingdotseq 243$, which is based on the overestimated assumption that 1% of all proteins could be regarded as potential binding proteins for the incednine. This *P*-value defines the probability that the prediction precision can be obtained by random selection of proteins. Then, *P*-value of 0.002 was obtained for the prediction precision 28.6%. This small *P*-value means that 28.6% (2/7) precision can be obtained with very small chance by random selection, and therefore, this small *P*-value proves the validity of our method.

Conclusions

Although further study is required for complete determination of the target protein of incednine, this study demonstrated that our proposed protocol of predicting target protein combining *in silico* screening and experimental verification is useful, and provides new insight into a strategy for identifying target proteins of small molecules.

Methods

Training datasets

The DrugBank dataset was constructed from Approved DrugCards data, which were downloaded from the DrugBank database [20]. These data consist of 964 approved drugs and their 456 associated target proteins, constituting 1,731 interacting pairs or positives. Additional data about 53 interactions with incednine, listed in Table 1, were obtained from our previous binding experiments.

Feature vectors

An amino acid sequence of protein is divided into trimers (three amino acid residues), and all of the 8,000 trimers are clustered into 199 groups according to physical-chemical properties. Then, an amino acid sequence is converted to a 199-dimensional feature vector based on the frequencies of 199 clusters (See for [13] the details of this procedure). A chemical compound is also converted to another feature vector of 199 dimension representing substructure statistics extracted from the structural formula of a chemical compound. The size of the dimensions, that is, 199 dimensions, was determined based on the variance of each dimension. The top 199 dimensions with significantly diverse variances in statistical classification were selected.

Statistical prediction method for protein-chemical interaction

We developed a comprehensively applicable statistical prediction method for interactions between any proteins

and chemical compounds, which requires only protein sequence data and chemical structure data and utilizes the statistical learning method of Support Vector Machines (SVM)[13,14].

We consider the problem as the binary classification of protein-chemical pairs whose abstractive identities are represented numerically by the 199 dimensional feature vectors defined above. We obtained a "positive" sample set, i.e., a set of protein-chemical pairs that have been proven to interact with each other via biological assays, from the DrugBank database [20]. Along with the positive sample set, SVM-based classifiers require a "negative" sample set, i.e., a set of protein-chemical pairs that do not interact with each other. Such a negative sample set can be extracted randomly from the whole complement set of the positive sample set. Though we used random pairs of drugs and proteins as negative samples in constructing a model, the lack of reliable negative samples is always a problem when applying the statistical learning methods. In our current study, it is assumed that drugs in the DrugBank dataset rarely interact with proteins other than their known targets because they are approved drugs. Using the resultant positive and negative protein-chemical pair sets, we trained two-layer SVMs. First, we trained each multiple first-layer SVM with small sample sets designed with different criteria. Next, using another larger sample set, we trained a second-layer SVM whose input is a set of probabilities output from the firstlayer SVMs. The prediction performances were evaluated by 10-fold cross-validation using the DrugBank dataset. The sensitivity, specificity, precision, and accuracy were 0.954, 0.999, 0.984, and 0.997, respectively, in cross-validation. The details of the algorithms and their prediction accuracy are described in our previous reports [13,14].

Support vector machines

Given n samples, each of which has an m-dimensional feature vector $\left(x_i = \left(x_i^1, \ldots, x_i^m\right)\right)$ and one of two classes, such as binding and non-binding $(y \in \{1, -1\})$, an SVM produces the classifier

$$f(x) = sign\left(\sum_{i=1}^{n} \alpha_i y_i K(x_i, x) + b\right),$$

where x is any new object which needs to be classified, $K(\cdot,\cdot)$ is a kernel function which indicates that the similarity between two vectors and $(\alpha_1, \cdots, \alpha_n)$ are the learned parameters. The RBF kernel $K(S_1, S_2) = \exp(-\gamma \| S_1 - S_2 \|)$ was utilized for the SVM classifier. In our study, the LIBSVM program [43] was employed to construct the SVM model.

Cell culture

Bcl-xL-overexpressing human SCLC Ms-1 cells [15] were maintained in Rosewell Park Memorial Institute media (Nissui, Japan) supplemented with 5% fetal bovine serum, 100 U/ml penicillin G, and 0.1 mg/mL kanamycin at 37°C in a humidified 5% CO_2 atmosphere.

Antibodies

Mouse monoclonal anti-DAPK1 (DAPK-55), rabbit monoclonal anti-PIK3CG (Y388), rabbit monoclonal anti-ACACA (EP687Y), mouse monoclonal anti-PIK3C2B, rabbit polyclonal anti-ITPR1, mouse monoclonal anti-PIP5K3, mouse monoclonal anti-CHD4, mouse polyclonal anti-GTF2IRD2, mouse polyclonal anti-PLCB1 antibodies were purchased from Abcam (Cambridge, MA). Rabbit polyclonal anti-KIF21B and mouse monoclonal anti-KIF5B (clone H2) antibodies were purchased from Millipore (Bedford, MA). Goat polyclonal anti-PARP14 and goat polyclonal anti-KIF1A were purchased from Santa Cruz Biotechnology (Santa Cruz, CA). Mouse monoclonal anti-Beclin (clone 20) antibody was purchased from BD Transduction Laboratories (San Diego, CA). Rabbit polyclonal anti-PARP1 antibody was purchased from Cell Signaling Technology (Beverly, MA). Rabbit polyclonal anti-RGPD5 antibody was purchased from Lifespan Biosciences (Seattle, WA). Mouse monoclonal anti-Flag (M2) antibody was purchased form Sigma (St. Louis, MO).

Horseradish peroxidase-conjugated anti-mouse IgG and anti-rabbit IgG secondary antibodies were purchased from GE Healthcare (Little Chalfont, UK). Horseradish peroxidase-conjugated anti-goat IgG was purchased from Santa Cruz Biotechnology.

Western blotting

Cell lysates were separated by SDS-PAGE and transferred to a PVDF membrane (Millipore) by electroblotting. After the membranes had been incubated with primary and secondary antibodies, the immune complexes were detected with an Immobilon Western kit (Millipore), and luminescence was detected with a LAS-1000 mini (Fujifilm, Tokyo, Japan).

Preparation of incednine and biotinylated incednine

Incednine was isolated from the culture broth of *Streptomyces* sp. ML694-90F3 [15]. To obtain biotinylated incednine (see Additional file 3), incednine (137.0 mg) and the amine-reactive biotin-X (100.0 mg; Invitrogen) were dissolved in 13.0 mL $CHCl_3$:MeOH (10:1). After stirring at 40°C for 20 h, the reaction mixture was concentrated to dryness. The residue was resolved in 50 mL $CHCl_3$:MeOH:H_2O (5:6:4) and partitioned three times under basic conditions. The lower layer of $CHCl_3$:MeOH:H_2O (5:6:4) was evaporated *in vacuo* to yield a brown residue. The residue was purified by HPLC

(Senshu Pak Pegasil ODS 30 x 250 mm) and eluted with MeOH:40 mM KH_2PO_4 aq. (70:30) to give 19.4 mg biotinylated incednine.

In vitro biotinylated incednine pull-down assay

Bcl-xL-overexpressiong Ms-1 cells were collected and sonicated twice in IP buffer (50 mM HEPES (pH 7.5), 150 mM NaCl, 2.5 mM EGTA, 1 mM EDTA, 1 mM DTT, and a protease inhibitor cocktail (Roche, Mannheim, Germany)) for 10 s. The cell lysates were centrifuged at 10,000*g* for 15 min at 4°C. The resulting supernatants were incubated with biotin (50 nmol) or biotinylated incednine (50 nmol) and avidin beads at 4°C for 3 h. The beads were washed three times with phosphate-buffered saline (PBS). The bound proteins were eluted with 2 mM biotin in PBS, and concentrated by a centrifugal filter device (Ultracel (YM-10); Millipore). The resulting proteins were boiled in SDS sample buffer for 5 min and subjected to western blotting.

Liquid chromatography-tandem mass spectrometry

Incednine binding proteins purified using biotinylated incednine / avidin beads, and flag-tagged incednine (see Additional file 4) / anti-Flag antibody were anaylzed by liquid chromatography-tandem mass spectrometry (LC–MS/MS) system as previously described, respectively [44,45].

Additional files

Additional file 1: Validation work for eIF4A3, PDI, PP2A and Hsp70.

Additional file 2: Proteins computationally predicted to bind to incednine (grouped into 11 clusters).

Additional file 3: A stucture of biotinylated incednine.

Additional file 4: Preparation of Flag-tagged Incednine [46,47].

Authors' contributions

YS and MI designed the study and analyzed the data. HK, HH, MN and YF performed the experiments. YS, MI and HK wrote the paper. YF synthesized biotinylated incednine. AI, MY, SI, KS, TD, TT, and TN performed MS/MS analysis. All authors read and approved the final manuscript.

Acknowledgements

This work was supported in part by a Grant program for bioinformatics research and development from the Japan Science and Technology Agency. This work was also supported by Grant-in-Aid for Scientific Research (A) No.23241066 from the Ministry of Education, Culture, Sports, Science and Technology of Japan.

Author details

[1]Department of Biosciences and Informatics, Faculty of Science and Technology, Keio University, 3-14-1 Hiyoshi, Kohoku-ku, Yokohama 223-8522, Japan. [2]Chemical Genetics Laboratory, RIKEN Advanced Science Institute, 2-1 Hirosawa, Wako-shi, Saitama 351-0198, Japan. [3]National Institute of Advanced Industrial Science and Technology (AIST), 2-4-7 Aomi, Koto-ku, Tokyo 135-0064, Japan. [4]Graduate School of Pharmaceutical Sciences, Tohoku University, 6-3 Aza-Aoba, Aramaki, Aoba, Sendai 980-8578, Japan. [5]Department of Applied Chemistry, Tokyo Institute of Technology, 2-12-1 Ookayama, Meguro, Tokyo 152-8552, Japan.

Received: 15 November 2011 Accepted: 5 April 2012
Published: 5 April 2012

References

1. Alaimo PJ, Shogren-Knaak MA, Shokat KM: **Chemical genetic approaches for the elucidation of signaling pathways.** *Curr Opin Chem Biol* 2001, **5**:360–367.
2. Zheng XF, Chan TF: **Chemical genomics in the global study of protein functions.** *Drug Discov Today* 2002, **7**:197–205.
3. Harding MW, Galat A, Uehling DE, Schreiber SL: **A receptor for the immunosuppressant FK506 is a cis-trans peptidyl-prolyl isomerase.** *Nature* 1989, **341**:758–760.
4. Liu J, Farmer JD Jr, Lane WS, Friedman J, Weissman I, Schreiber SL: **Calcineurin is a common target of cyclophilin-cyclosporin A and FKBP-FK506 complexes.** *Cell* 1991, **66**:807–815.
5. Flanagan WM, Corthesy B, Bram RJ, Crabtree GR: **Nuclear association of a T-cell transcription factor blocked by FK-506 and cyclosporin A.** *Nature* 1991, **352**:803–807.
6. Nishi K, Yoshida M, Fujiwara D, Nishikawa M, Horinouchi S, Beppu T: **Leptomycin B targets a regulatory cascade of crm1, a fission yeast nuclear protein, involved in control of higher order chromosome structure and gene expression.** *J Biol Chem* 1994, **269**:6320–6324.
7. Kudo N, Matsumori N, Taoka H, Fujiwara D, Schreiner EP, Wolff B, Yoshida M, Horinouchi S: **Leptomycin B inactivates CRM1/exportin 1 by covalent modification at a cysteine residue in the central conserved region.** *Proc Natl Acad Sci U S A* 1999, **96**:9112–9117.
8. Yoshida M, Kijima M, Akita M, Beppu T: **Potent and specific inhibition of mammalian histone deacetylase both in vivo and in vitro by trichostatin A.** *J Biol Chem* 1990, **265**:17174–17179.
9. Whitesell L, Mimnaugh EG, De Costa B, Myers CE, Neckers LM: **Inhibition of heat shock protein HSP90-pp 60v-src heteroprotein complex formation by benzoquinone ansamycins: essential role for stress proteins in oncogenic transformation.** *Proc Natl Acad Sci U S A* 1994, **91**:8324–8328.
10. Stebbins CE, Russo AA, Schneider C, Rosen N, Hartl FU, Pavletich NP: **Crystal structure of an Hsp90-geldanamycin complex: targeting of a protein chaperone by an antitumor agent.** *Cell* 1997, **89**:239–250.
11. Prodromou C, Roe SM, O'Brien R, Ladbury JE, Piper PW, Pearl LH: **Identification and structural characterization of the ATP/ADP-binding site in the Hsp90 molecular chaperone.** *Cell* 1997, **90**:65–75.
12. Hart CP: **Finding the target after screening the phenotype.** *Drug Discov Today* 2005, **10**:513–519.
13. Nagamine N, Sakakibara Y: **Statistical prediction of protein chemical interactions based on chemical structure and mass spectrometry data.** *Bioinformatics* 2007, **23**:2004–2012.
14. Nagamine N, Shirakawa T, Minato Y, Torii K, Kobayashi H, Imoto M, Sakakibara Y: **Integrating statistical predictions and experimental verifications for enhancing protein-chemical interaction predictions in virtual screening.** *PLoS Comput Biol* 2009, **5**:e1000397.
15. Futamura Y, Sawa R, Umezawa Y, Igarashi M, Nakamura H, Hasegawa K, Yamasaki M, Tashiro E, Takahashi Y, Akamatsu Y, *et al*: **Discovery of incednine as a potent modulator of the anti-apoptotic function of Bcl-xL from microbial origin.** *J Am Chem Soc* 2008, **130**:1822–1823.
16. Michelle L, Cloutier A, Toutant J, Shkreta L, Thibault P, Durand M, Garneau D, Gendron D, Lapointe E, Couture S, *et al*: **Proteins Associated with the Exon Junction Complex Also Control the Alternative Splicing of Apoptotic Regulators.** *Mol Cell Biol* 2012, **32**:954–967.
17. Lovat PE, Corazzari M, Armstrong JL, Martin S, Pagliarini V, Hill D, Brown AM, Piacentini M, Birch-Machin MA, Redfern CP: **Increasing melanoma cell death using inhibitors of protein disulfide isomerases to abrogate survival responses to endoplasmic reticulum stress.** *Cancer Res* 2008, **68**:5363–5369.
18. Didelot C, Lanneau D, Brunet M, Joly AL, De Thonel A, Chiosis G, Garrido C: **Anti-cancer therapeutic approaches based on intracellular and extracellular heat shock proteins.** *Curr Med Chem* 2007, **14**:2839–2847.
19. Lu J, Kovach JS, Johnson F, Chiang J, Hodes R, Lonser R, Zhuang Z: **Inhibition of serine/threonine phosphatase PP2A enhances cancer chemotherapy by blocking DNA damage induced defense mechanisms.** *Proc Natl Acad Sci U S A* 2009, **106**:11697–11702.
20. Wishart DS, Knox C, Guo AC, Shrivastava S, Hassanali M, Stothard P, Chang Z, Woolsey J: **DrugBank: a comprehensive resource for in silico drug discovery and exploration.** *Nucleic Acids Res* 2006, **34**:D668–D672. Database issue.

21. Stephens LR, Eguinoa A, Erdjument-Bromage H, Lui M, Cooke F, Coadwell J, Smrcka AS, Thelen M, Cadwallader K, Tempst P, *et al*: **The G beta gamma sensitivity of a PI3K is dependent upon a tightly associated adaptor, p101.** *Cell* 1997, **89**:105–114.
22. Engelman JA, Luo J, Cantley LC: **The evolution of phosphatidylinositol 3-kinases as regulators of growth and metabolism.** *Nat Rev Genet* 2006, **7**:606–619.
23. Hickey FB, Cotter TG: **BCR-ABL regulates phosphatidylinositol 3-kinase-p110gamma transcription and activation and is required for proliferation and drug resistance.** *J Biol Chem* 2006, **281**:2441–2450.
24. Edling CE, Selvaggi F, Buus R, Maffucci T, Di Sebastiano P, Friess H, Innocenti P, Kocher HM, Falasca M: **Key role of phosphoinositide 3-kinase class IB in pancreatic cancer.** *Clin Cancer Res* 2010, **16**:4928–4937.
25. Ame JC, Spenlehauer C, de Murcia G: **The PARP superfamily.** *Bioessays* 2004, **26**:882–893.
26. Kim MY, Zhang T, Kraus WL: **Poly(ADP-ribosyl)ation by PARP-1: 'PAR-laying' NAD + into a nuclear signal.** *Genes Dev* 2005, **19**:1951–1967.
27. Herceg Z, Wang ZQ: **Functions of poly(ADP-ribose) polymerase (PARP) in DNA repair, genomic integrity and cell death.** *Mutat Res* 2001, **477**:97–110.
28. Wang ZQ, Stingl L, Morrison C, Jantsch M, Los M, Schulze-Osthoff K, Wagner EF: **PARP is important for genomic stability but dispensable in apoptosis.** *Genes Dev* 1997, **11**:2347–2358.
29. Helleday T, Petermann E, Lundin C, Hodgson B, Sharma RA: **DNA repair pathways as targets for cancer therapy.** *Nat Rev Cancer* 2008, **8**:193–204.
30. Farmer H, McCabe N, Lord CJ, Tutt AN, Johnson DA, Richardson TB, Santarosa M, Dillon KJ, Hickson I, Knights C, *et al*: **Targeting the DNA repair defect in BRCA mutant cells as a therapeutic strategy.** *Nature* 2005, **434**:917–921.
31. Albert JM, Cao C, Kim KW, Willey CD, Geng L, Xiao D, Wang H, Sandler A, Johnson DH, Colevas AD, *et al*: **Inhibition of poly(ADP-ribose) polymerase enhances cell death and improves tumor growth delay in irradiated lung cancer models.** *Clin Cancer Res* 2007, **13**:3033–3042.
32. Veuger SJ, Curtin NJ, Richardson CJ, Smith GC, Durkacz BW: **Radiosensitization and DNA repair inhibition by the combined use of novel inhibitors of DNA-dependent protein kinase and poly(ADP-ribose) polymerase-1.** *Cancer Res* 2003, **63**:6008–6015.
33. Yu SW, Wang H, Poitras MF, Coombs C, Bowers WJ, Federoff HJ, Poirier GG, Dawson TM, Dawson VL: **Mediation of poly(ADP-ribose) polymerase-1-dependent cell death by apoptosis-inducing factor.** *Science* 2002, **297**:259–263.
34. Cregan SP, Dawson VL, Slack RS: **Role of AIF in caspase-dependent and caspase-independent cell death.** *Oncogene* 2004, **23**:2785–2796.
35. Hong SJ, Dawson TM, Dawson VL: **Nuclear and mitochondrial conversations in cell death: PARP-1 and AIF signaling.** *Trends Pharmacol Sci* 2004, **25**:259–264.
36. Menendez JA, Lupu R: **Fatty acid synthase and the lipogenic phenotype in cancer pathogenesis.** *Nat Rev Cancer* 2007, **7**:763–777.
37. Brusselmans K, De Schrijver E, Verhoeven G, Swinnen JV: **RNA interference-mediated silencing of the acetyl-CoA-carboxylase-alpha gene induces growth inhibition and apoptosis of prostate cancer cells.** *Cancer Res* 2005, **65**:6719–6725.
38. Chajes V, Cambot M, Moreau K, Lenoir GM, Joulin V: **Acetyl-CoA carboxylase alpha is essential to breast cancer cell survival.** *Cancer Res* 2006, **66**:5287–5294.
39. Wang C, Xu C, Sun M, Luo D, Liao DF, Cao D: **Acetyl-CoA carboxylase-alpha inhibitor TOFA induces human cancer cell apoptosis.** *Biochem Biophys Res Commun* 2009, **385**:302–306.
40. Beckers A, Organe S, Timmermans L, Scheys K, Peeters A, Brusselmans K, Verhoeven G, Swinnen JV: **Chemical inhibition of acetyl-CoA carboxylase induces growth arrest and cytotoxicity selectively in cancer cells.** *Cancer Res* 2007, **67**:8180–8187.
41. Milgraum LZ, Witters LA, Pasternack GR, Kuhajda FP: **Enzymes of the fatty acid synthesis pathway are highly expressed in in situ breast carcinoma.** *Clin Cancer Res* 1997, **3**:2115–2120.
42. Swinnen JV, Vanderhoydonc F, Elgamal AA, Eelen M, Vercaeren I, Joniau S, Van Poppel H, Baert L, Goossens K, Heyns W, *et al*: **Selective activation of the fatty acid synthesis pathway in human prostate cancer.** *Int J Cancer* 2000, **88**:176–179.
43. Chang C-C, Lin C-J: **LIBSVM: A library for support vector machines.** *ACM Trans Intell Syst Technol* 2011, **2**:1–27.
44. Kaida D, Motoyoshi H, Tashiro E, Nojima T, Hagiwara M, Ishigami K, Watanabe H, Kitahara T, Yoshida T, Nakajima H, *et al*: **Spliceostatin A targets SF3b and inhibits both splicing and nuclear retention of pre-mRNA.** *Nat Chem Biol* 2007, **3**:576–583.
45. Natsume T, Yamauchi Y, Nakayama H, Shinkawa T, Yanagida M, Takahashi N, Isobe T: **A direct nanoflow liquid chromatography-tandem mass spectrometry system for interaction proteomics.** *Anal Chem* 2002, **74**:4725–4733.
46. Tornøe CW, Chirstensen C, Meldal MJ: *Org Chem* 2002, **67**:3057–3064.
47. Rostovtsev VV, Green LG, Fokin VV, Sharpless KB: *Angew Chem Int Ed* 2002, **41**:2596–2599.

doi:10.1186/1472-6769-12-2
Cite this article as: Kobayashi *et al.*: Comprehensive predictions of target proteins based on protein-chemical interaction using virtual screening and experimental verifications. *BMC Chemical Biology* 2012 **12**:2.

Journal of Antibiotics (2012) 00, 1–6

www.nature.com/ja

ORIGINAL ARTICLE

Inostamycin enhanced TRAIL-induced apoptosis through DR5 upregulation on the cell surface

Kohta Yamamoto[1], Masafumi Makino[1], Ramida Watanapokasin[2], Etsu Tashiro[1] and Masaya Imoto[1]

Tumor necrosis factor-related apoptosis-inducing ligand (TRAIL) has been considered as a possible therapeutic agent for cancer treatment. This is because of its selective cytotoxicity against various cancer cells without a detrimental effect on normal cells. However, recent studies have reported that the potential application of TRAIL in cancer therapy is limited, as many cancer cells have been found to be resistant to TRAIL. Therefore, small molecule compounds that potentiate the cytotoxicity of TRAIL would be strategic candidates for therapeutic applications in combination with TRAIL. Here we found that a combined treatment of inostamycin and TRAIL synergistically induced caspase-dependent apoptosis in HCT116 cells. Inostamycin upregulated DR5, and a knockdown of DR5 suppressed the apoptosis that was synergistically induced by co-treatment with inostamycin and TRAIL. Moreover, inostamycin increased the expression of DR5 on the cell surface. Therefore, inostamycin-increased cell surface expression of DR5 may have contributed to the enhancement of TRAIL-induced apoptosis. Our study suggests that combined treatment with inostamycin and TRAIL may offer a strategy to overcome TRAIL resistance in tumor cells.
The Journal of Antibiotics advance online publication, 4 April 2012; doi:10.1038/ja.2012.21

Keywords: apoptosis; DR5; inostamycin; TRAIL

INTRODUCTION

Tumor necrosis factor-related apoptosis-inducing ligand (TRAIL), also known as Apo2L, is a type II transmembrane protein. TRAIL was originally identified on the basis of sequence homology to the Fas ligand and tumor necrosis factor.[1,2] TRAIL is hypothesized as being a potentially good therapeutic agent for cancer treatment. This is because TRAIL has been shown to induce apoptosis in a variety of tumor cell lines more efficiently than in normal cells.[3–5] TRAIL exerts its function by binding its receptors, which are expressed on the surface of target cells. To date, four different types of membrane-bound death receptors for TRAIL has been identified: TRAIL-R1/DR4, TRAIL-R2/DR5, TRAIL-R3/DcR1 and TRAIL-R4/DcR2. Both DR4 and DR5 have a conserved cytoplasmic region called the 'death domain'. This is a homolog to Fas and tumor necrosis factor-R1, and is required for TRAIL-induced apoptosis.[6–8] On the other hand, TRAIL also binds to DcR1 and DcR2 that sequester the ligand, but are unable to initiate an apoptosis signal. Thus, DcR1 and DcR2 are considered to be the decoy receptors.[7,9] The apoptosis signal that is induced by TRAIL has been shown to be similar to that which is induced by Fas. The TRAIL homotrimer induces trimerization of DR5 or DR4 on the surface of target cells, which leads to the formation of death-inducing signaling complex. The trimerization of the death domains results in the recruitment of an adaptor molecule Fas-associated protein with death domain (FADD), which in turn recruits and activates caspase-8. In type I cells, activation of caspase- 8 is sufficient for the subsequent activation of effector caspase-3. On the other hand, in type II cells, amplification through the mitochondrial pathway is initiated by the cleavage of Bid by caspase-8. Truncated-Bid causes the loss of mitochondrial membrane potential and caspase-9 cleavage, resulting in the activation of caspase-3 and subsequent cellular apoptosis.

The potential application of TRAIL in cancer therapy is currently limited, as many cancer cells have been found to be resistant to the cytotoxic effects of TRAIL. This resistance may be because of the low expression of pro-apoptotic molecules: death receptors or caspase-8. Alternatively, the resistance may be because of the high expression of anti-apoptotic molecules: decoy receptors, FLICE-like-inhibitory protein, inhibitor of apoptosis protein and Bcl-2. Because of the limitations of TRAIL-induced cytotoxicity, the combination of TRAIL with other small molecule compounds has been postulated as strategy to potentiate the cytotoxicity of TRAIL and its therapeutic applications. Indeed, it was reported that several chemotherapeutic agents and natural products, such as CDDP,[10] etoposide,[10,11] doxorubicin,[12] PS-341 (bortezomib),[13] tunicamycin,[14] rottlerin,[15] brandisianins,[16] silibinin[17] and sodium butyrate,[18] were succeeded to cause the sensitization of TRAIL-resistant tumor cells to TRAIL-induced apoptosis.

In this study, we have screened candidate small molecule compounds that synergistically induce apoptosis in the presence of

[1]Department of Biosciences and Informatics, Faculty of Science and Technology, Keio University, Yokohama, Japan and [2]Department of Biochemistry, Faculty of Medicine, Srinakharinwirot University, Bangkok, Thailand
Correspondence: Dr E Tashiro, Department of Biosciences and Informatics, Faculty of Science and Technology, Keio University, 3-14-1 Hiyoshi, Kohoku-ku, Yokohama, 223-8522, Japan.
E-mail: tashiro@bio.keio.ac.jp
Received 11 January 2012; revised 19 February 2012; accepted 27 February 2012

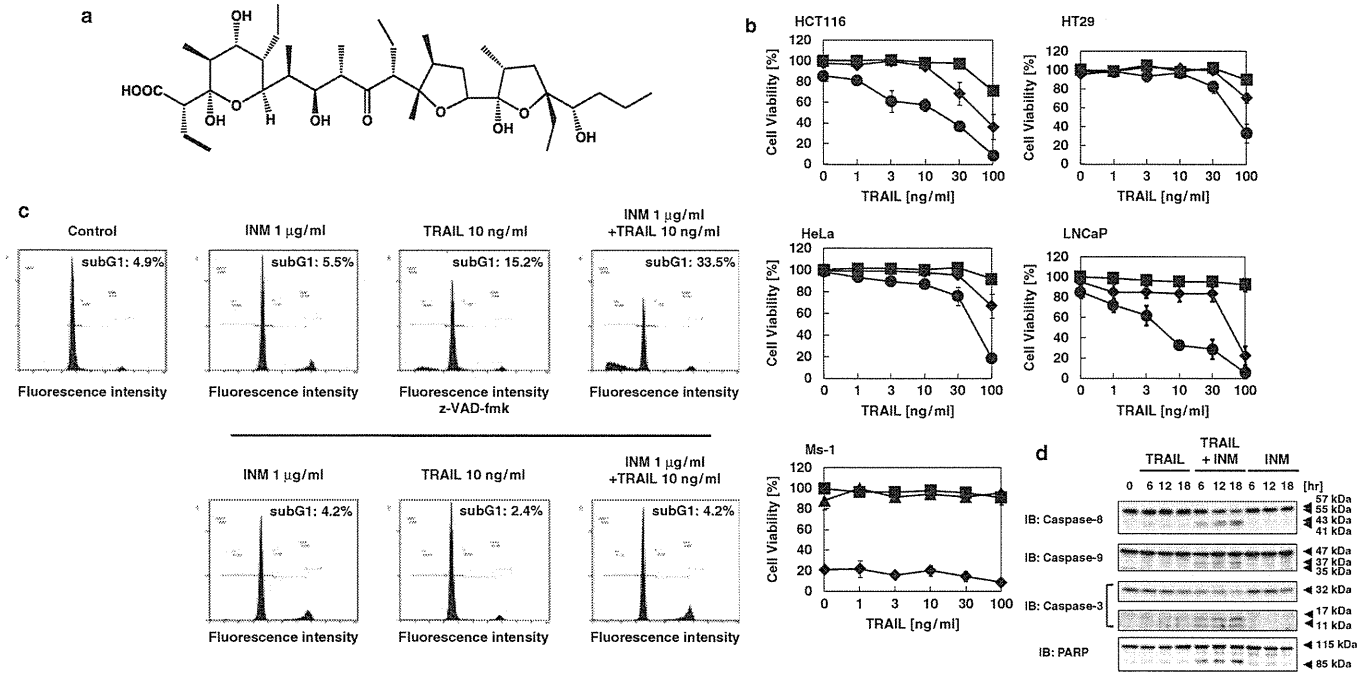

Figure 1 Co-treatment with inostamycin (INM) and tumor necrosis factor-related apoptosis-inducing ligand (TRAIL) synergistically induced apoptosis in HCT116 cells. (**a**) Structure of inostamycin.[19] (**b**) Co-treatment with INM and TRAIL induced a synergistic cytotoxicity in HCT116 cells, HeLa cells, HT29 cells and LNCaP cells, but not in Ms-1 cells. HCT116 cells, HeLa cells, HT29 cells, LNCaP cells or Ms-1 cells were treated with the indicated concentration of TRAIL and 0.0 (square), 0.01 (triangle), 0.1 (diamond-shaped) or 1 (circle) $\mu g\,ml^{-1}$ of INM for 18 h. The cytotoxicity was evaluated using a Trypan Blue Exclusion assay. (**c**) The cytotoxicity induced by the co-treatment with INM and TRAIL was completely suppressed by z-VAD-fmk. HCT116 cells were pre-treated with or without 100 μM of z-VAD-fmk, and then treated further with 10 $ng\,ml^{-1}$ of TRAIL and 1 $\mu g\,ml^{-1}$ of INM. After an 18-h incubation period, the sub-G_1 population was measured by flow cytometer. (**d**) Co-treatment with INM and TRAIL activated caspase. HCT116 cells were treated with or without 10 $ng\,ml^{-1}$ of TRAIL and 1 $\mu g\,ml^{-1}$ of INM for the indicated periods. Cell extracts were prepared for western blotting to detect the expression of caspase-8, caspase-9, caspase-3 and poly(ADP-ribose) polymerase (PARP).

TRAIL. As a result, we found that co-treatment with inostamycin and TRAIL synergistically induced caspase-dependent apoptosis in colorectal cancer HCT116 cells. Inostamycin was isolated from *Streptomyces* species. MH816-AF15;[19] its structure was shown in Figure 1a. Inostamycin weakly upregulated DR4 and strongly upregulated DR5 expression. Additionally, the synergistic apoptosis that was induced by this co-treatment was completely suppressed in DR5 small interfering RNA (siRNA)-transfected but not in DR4 siRNA-transfected HCT116 cells. Furthermore, inostamycin increased cell surface expression of DR5. Taken together with these results, upregulation of cell surface DR5 by inostamycin possibly contributes to the enhancement of TRAIL-induced apoptosis.

MATERIALS AND METHODS

Materials

Inostamycin was prepared as previously described,[19] TRAIL was purchased from Millipore (Billerica, MA, USA). Tunicamycin and z-VAD-fmk were purchased from SIGMA (St. Louis, MO, USA). Rabbit monoclonal anti-poly(ADP-ribose) polymerase, rabbit polyclonal anti-caspase-9, anti-caspase-3, anti-Bcl-xL and mouse monoclonal anti-caspase-8 were purchased from Cell Signaling Technology (Beverly, MA, USA). Rabbit polyclonal anti-survivin was purchased from Santa Cruz Biotechnology (Santa Cruz, CA, USA). Mouse monoclonal anti-X-linked inhibitor of apoptosis protein (XIAP) was purchased from BD Transduction Laboratories (San Diego, CA, USA). Mouse monoclonal anti-Bcl-2 was purchased from Dako (Carpentaria, CA, USA). Rabbit polyclonal anti-DR5 was purchased from Proscience (Poway, CA, USA). Rabbit polyclonal anti-DR4 was purchased from Millipore. Mouse monoclonal anti-C/EBP homologous protein (CHOP) was purchased from Thermo scientific (Rockford, IL, USA). Mouse monoclonal anti-DR5 phycoerythrin (PE)-conjugated was purchased from eBioscience (San Diego, CA, USA). Horseradish peroxidase-conjugated anti-mouse IgG and anti-rabbit IgG secondary antibodies were purchased from GE Healthcare (Little Chalfont, UK).

Cell culture

Human colorectal carcinoma HCT116 cells, HT29 cells and human small cell lung cancer Ms-1 cells were maintained in Roswell Park Memorial Institute medium (Nissui, Tokyo, Japan) supplemented with 5% fetal bovine serum. Human cervical cancer HeLa cells were maintained in Dulbecco's modified Eagle's medium (Nissui, Tokyo, Japan) supplemented with 8% fetal bovine serum. Human prostate adenocarcinoma LNCaP cells were maintained in Roswell Park Memorial Institute medium supplemented with 10% fetal bovine serum— Roswell Park Memorial Institute medium.

Trypan blue exclusion assay

HCT116 cells, HT29 cells, HeLa cells, LNCaP cells or Ms−1 cells were seeded in 48-well plates and incubated overnight, before experiments were conducted. The cells were treated with TRAIL with or without inostamycin for 18 h. Floating and adherent cells were collected and resuspended in phosphate-buffered saline (PBS^-). Cells were mixed with trypan blue and counted under the microscope.

Propidium iodide staining

Propidium iodide staining and flow cytometry were used to determine the degree of cellular apoptosis. HCT116 cells were seeded in 6-well plates and incubated overnight before experiment. The cells were treated with TRAIL with or without inostamycin for 18 h. Floating and adherent cells were collected and resuspended in PBS^-. Cold ethanol was added in a dropwise manner while vortexing to fix the cells. Fixed cells were collected and resuspended in PBS^- containing 50 $\mu g\,ml^{-1}$ propidium iodide. Flow cytometry was done using

EPICS (Beckman Coulter, Fullerton CA, USA). The percentage of sub-G_1 cells was used to quantify apoptotic cells.

Western blotting

Cells were lysed with a lysis buffer containing 25 mM HEPES (pH 7.8), 1.5% Triton-X 100, 1.0% sodium deoxycholate, 0.1% SDS, 0.5 M NaCl, 5 mM EDTA, 50 mM NaF, 100 μM Na_3VO_4, 0.1 mg ml^{-1} leupeptin and 1 mM phenylmethylsulfonyl fluoride. Proteins were separated by SDS—polyacryalamide gel electrophoresis and transferred to a polyvinylidene fluoride membrane (Millipore). After the membranes had been incubated with primary and secondary antibodies, the immune complexes were detected with an Immobilon Western kit (Millipore), and the luminescence was detected with a LAS-1000 mini (Fujifilm, Tokyo, Japan).

Real-time reverse transcriptase (RT)–PCR analysis

Total RNA was isolated with TRIzol (Invitrogen, Carlsbad, CA, USA). Reverse transcription was performed with M-MLV reverse transcriptase (PROMEGA, Madison, WI, USA) according to the manufacturer's instructions. Real-time reverse transcription (RT)–PCR was performed using SYBR Premix Ex Taq (Takara, Shiga, Japan). Primer sequence was as follows: DR5, 5′-CACCA GGTGTGATTCAGGTG-3′ (sense) and 5′-TACGGCTGCAACTGTGACTC-3′ (antisense); CHOP, 5′-GCGCATGAAGGAGAAAGAAC-3′ (sense) and 5′-TCACCATTCGGTCAATCAGA-3′ (antisense); glyceraldehyde-3-phosphate dehydrogenase, 5′-AGGTCGGAGTCAACGGATTT-3′ (sense) and 5′-TAGTTG AGGTCAATGAAGGG-3′ (antisense).

RNA interference

siRNA for control (12935-300), CHOP (5′-CCUCACUCUCCAGAUUCCA GUCAGA-3′) DR4 (HSS112945) and DR5 (HSS112939) were purchased from Invitrogen. HCT116 cells were transfected with siRNA using HiPerFect (QIAGEN, Hilden, Germany), according to the manufacturer's instructions.

Cell surface staining of DR5

HCT116 cells were seeded in 6-well plates and incubated overnight before the experiment. Cells were then treated with inostamycin for 12 h. Cells were then collected and resuspended in PBS$^-$ including PE-conjugated DR5 antibody. After incubation for 1 h at 4 °C, the cells were washed with PBS$^-$ twice and resuspended in PBS$^-$. Flow cytometry analysis was performed with EPICS (Beckman Coulter).

RESULTS AND DISCUSSION

Co-treatment with inostamycin and TRAIL synergistically induced apoptosis in HCT116 cells

In this study, we first found that co-treatment with inostamycin and TRAIL synergistically induced cytotoxicity in HCT116 cells. As shown in Figure 1b, although neither 10 ng ml^{-1} TRAIL nor 1 μg ml^{-1} inostamycin alone showed cytotoxicity in HCT116 cells after 18 h treatment, the cell viability was decreased to about 40% when HCT116 cells were treated with inostamycin and TRAIL in combination. The synergistic cytotoxicity occurred in inostamycin and TRAIL dose-dependent manner. This synergistic effect is cell type-dependent, and is observed in HeLa cells, HT29 cells and LNCaP cells but not in Ms-1 cells (Figure 1b). Flow cytometer analysis demonstrated that the synergistic increase of the Sub-G_1 population was observed in co-treatment with inostamycin and TRAIL in HCT116 cells (Figure 1c). Furthermore, a one hour preincubation with the pan-caspase inhibitor 100 μM z-VAD-fmk suppressed the cell death that was induced by co-treatment with inostamycin and TRAIL (Figure 1c). We also observed the cleavage of caspase-8, caspase-9, caspase-3 and poly(ADP-ribose) polymerase, a well known substrate of caspase-3, at 6 h after inostamycin and TRAIL co-treatment (Figure 1d). In contrast, the cleaved caspase-8, caspase-9, caspase-3 and poly(ADP-ribose) polymerase were only weakly detected when HCT116 cells were treated with 10 ng ml^{-1} of TRAIL alone. Inostamycin alone also could not activate caspase-8, caspase-9 or caspase-3 in HCT116 cells (Figure 1d). These results suggested that co-treatment with inostamycin and TRAIL induced caspase-dependent apoptosis.

Inostamycin enhanced TRAIL-induced apoptosis possibly through DR5 upregulation on the cell surface

TRAIL-stimulated death signal is initiated by the binding of TRAIL to DR4 or DR5, which resulted in the subsequent activation of caspase-8. As shown in Figure 2a, western blotting analysis using an anti-DR4 or anti-DR5 antibody showed that inostamycin strongly upregulated the DR5 protein in HCT116 cells, it also slightly upregulated the DR4 protein (Figure 2a). Similarly, inostamycin-induced DR5 upregulation was also observed in HT29 cells and HeLa cells, in which co-treatment with inostamycin and TRAIL induced synergistic cytotoxicity (Figure 2a). Inostamycin-induced DR5 protein was detected as two bands, which were likely products of alternative splice variants of the DR5 gene[20,21] Furthermore, under the condition where inostamycin-upregulated DR4 or -DR5 protein was efficiently reduced by transient transfection of DR4 siRNA or DR5 siRNA (Figure 2b), apoptosis induced by co-treatment with inostamycin and TRAIL was completely suppressed in DR5 siRNA-transfected HCT116 cells, but not in DR4 siRNA-transfected HCT116 cells (Figure 2c). These results indicated that DR5 is indispensable for the apoptosis induced by co-treatment with inostamycin and TRAIL. Moreover, inostamycin induced cell surface expression of DR5 in a time-dependent manner (Figure 2d). On the other hand, the protein expression of four anti-apoptotic molecules, Bcl-2, Bcl-xL, XIAP and survivin, was unaffected by inostamycin in HCT116 cells (Figure 2e). Considering that it increases the cell surface expression of DR5, it is likely that inostamycin-increased cell surface expression of DR5 contributes to TRAIL sensitization.

Inostamycin-induced transcription of DR5 was regulated by CHOP.

As shown in Figure 3a, inostamycin-induced increases in DR5 mRNA levels were evaluated by real-time RT–PCR analysis. This data suggests that inostamycin activates transcription of DR5 in HCT116 cells. Recent studies have reported that tunicamycin-induced[14] and MG132-induced[22] CHOP (C/EBP homologous protein) upregulation activates DR5 transcription through CHOP-binding site in DR5 promoter region. This results in a sensitization of TRAIL-induced apoptosis. As we also found that 1 μg ml^{-1} inostamycin increased CHOP protein expression with similar time-course kinetics to DR5 upregulation (Figure 3b), we next examined whether this inostamycin-induced CHOP expression regulated DR5 transcription. When CHOP was successfully silenced by transient transfection of siRNA for CHOP (siCHOP) (Figure 3c), inostamycin-increased DR5 mRNA was markedly suppressed (Figure 3d). Furthermore, as consistent with previous report, tunicamycin-increased expression of DR5 mRNA was also completely suppressed in siCHOP-transfected HCT116 cells (Figure 3d). Next, we examined whether inostamycin-induced DR5 protein upregulation was also suppressed in CHOP-knockdown HCT116 cells. As shown in Figures 4a and b, neither inostamycin-induced DR5 protein expression nor inostamycin-increased cell surface expression of DR5 was suppressed under the conditions where tunicamycin-induced DR5 protein expression was completely suppressed in CHOP-knockdown cells. Furthermore, the transient transfection with siCHOP could not suppress apoptosis induction by the synergistic effect of co-treatment with inostamycin and TRAIL (Figure 4c).

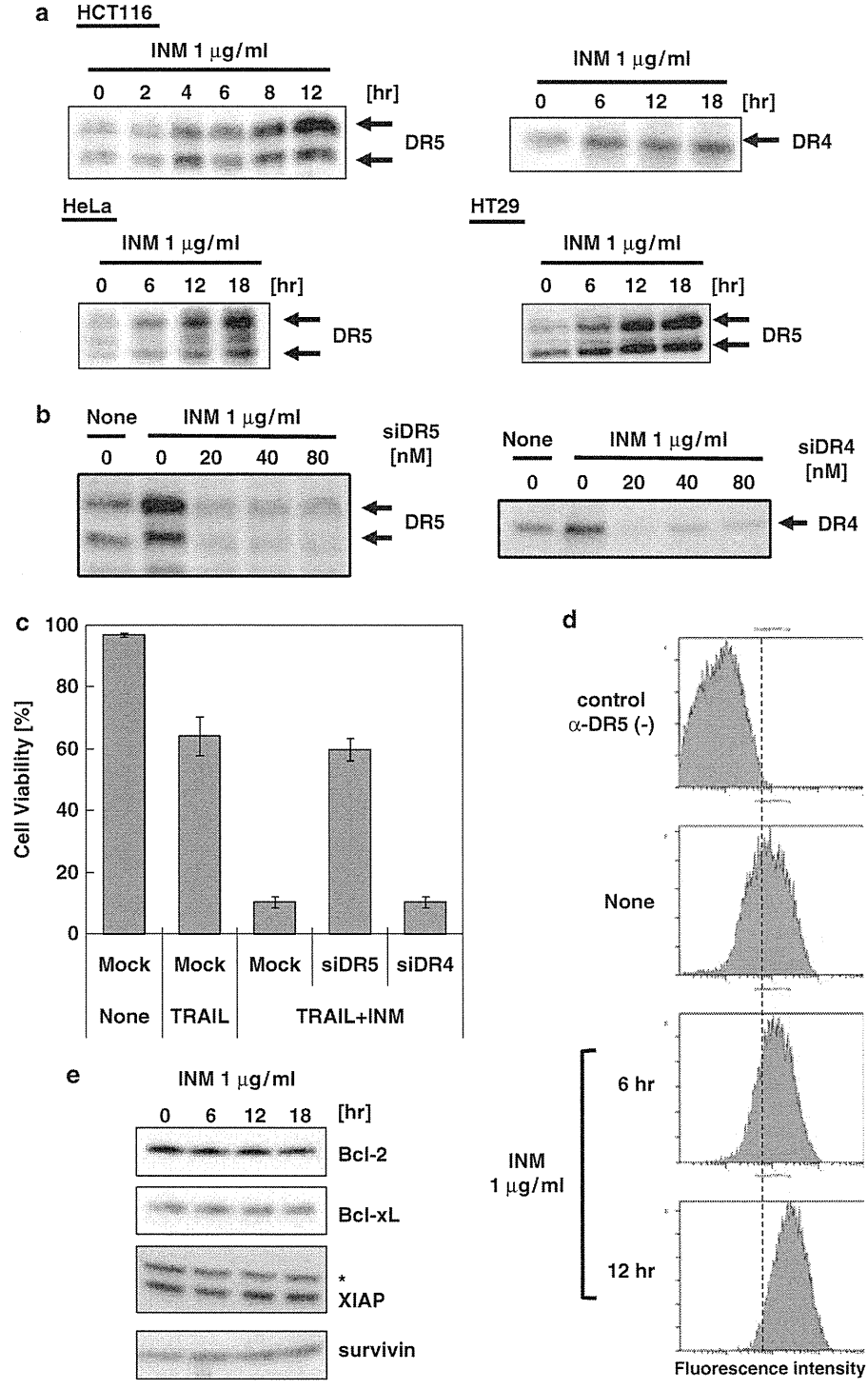

Figure 2 Inostamycin (INM) increased cell surface expression of DR5 in HCT116 cells. (**a**) Effect of INM on the expression of DR4 and DR5 in HCT116 cells, and DR5 in HeLa cells and HT29 cells. HCT116 cells, HeLa cells and HT29 cells were treated with 1 μg ml^{-1} of INM for the indicated periods. Cell extracts were prepared for western blotting to detect the expression of DR4 and DR5. (**b**) Transient transfection of small interfering RNA (siRNA) against DR4 or DR5 suppressed INM-induced DR4 or DR5 expression in HCT116 cells. HCT116 cells were transiently transfected with the indicated concentration of DR4 siRNA (siDR4) or DR5 siRNA (siDR5). After incubation for 24 h, the transfected cells were treated with 1 μg ml^{-1} of INM for 12 h. Cell extracts were prepared for western blotting to detect the expression of DR4 and DR5. (**c**) Knockdown of DR5 suppressed synergistic apoptosis induction by co-treatment with INM and tumor necrosis factor-related apoptosis-inducing ligand (TRAIL). HCT116 cells were transiently transfected with 20 nM DR4 siRNA (siDR4) or siDR5. After incubation for 24 h, the transfected cells were treated with or without 1 μg ml^{-1} INM together with 10 ng ml^{-1} TRAIL for more 24 h. The cell viability was evaluated using a Trypan Blue Exclusion assay. (**d**) INM increased the cell surface expression of DR5 in HCT116 cells. HCT116 cells were treated with 1 μg ml^{-1} of INM for 6 or 12 h. The cell surface DR5 were stained with or without PE-conjugated DR5 antibody and then further detected with flow cytometer. (**e**) INM did not affect the expression of anti-apoptotic proteins in HCT116 cells. HCT116 cells were treated with 1 μg ml^{-1} of INM for the indicated periods. Cell extracts were prepared for western blotting to detect the expression of Bcl-2, Bcl-xL, XIAP and survivin. * indicates non-specific band.

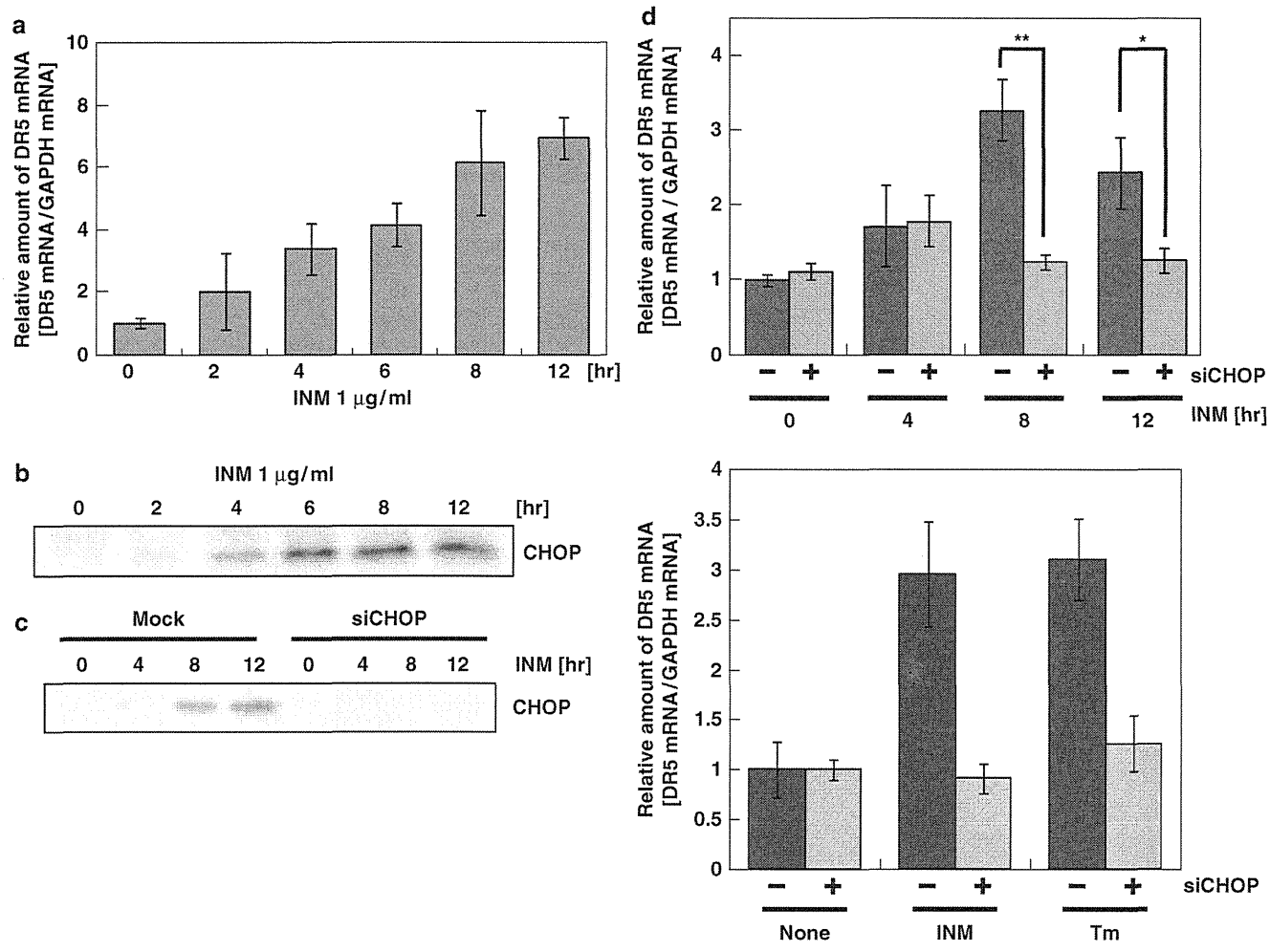

Figure 3 Inostamycin (INM) activated DR5 transcription through CHOP upregulation. (**a**) INM induced DR5 upregulation of mRNA levels in HCT116 cells. HCT116 cells were treated with 1 μg ml^{-1} of INM for the indicated periods. The cells were collected and RNA was extracted. DR5 mRNA levels were evaluated by real-time RT–PCR. DR5 mRNA was normalized with the mRNA levels of glyceraldehyde-3-phosphate dehydrogenase. Data are the means ± s.d. among three independent experiments. (**b**) Effect of INM on the expression of CHOP in HCT116 cells. HCT116 cells were treated with 1 μg ml^{-1} of INM for the indicated periods. Cell extracts were prepared for western blotting to detect the expression of CHOP. (**c**) Transient transfection of small interfering RNA (siRNA) against CHOP suppressed INM-induced CHOP expression in HCT116 cells. HCT116 cells were transiently transfected with 20 nM siCHOP. After 24 h incubation, the transfected cells were treated with 1 μg ml^{-1} of INM for 4, 8 or 12 h. Cell extracts were prepared for western blotting to detect the expression of CHOP. (**d**) Knockdown of CHOP suppressed INM- and tunicamycin (Tm)-induced DR5 upregulation at mRNA levels. HCT116 cells were transiently transfected with 20 nM siCHOP. After incubation for 24 h, the transfected cells were treated with 1 μg ml^{-1} of INM for 4, 8 or 12 h or 10 μg ml^{-1} of Tm for 12 h. The cells were collected and RNA was extracted. DR5 mRNA levels were evaluated by real-time RT–PCR. DR5 mRNA was normalized with the mRNA levels of glyceraldehyde-3-phosphate dehydrogenase (GAPDH). Data are the means ± s.d. among three independent experiments. *P<0.05 and **P<0.005.

When considered together, our results suggest that inostamycin enhanced TRAIL-induced apoptosis possibly because of a CHOP-independent upregulation of DR5 on the cell surface. At present, the mechanism by which inostamycin upregulates DR5 protein expression remains unclear. However, these results were consistent with our conclusion that the inostamycin-increased cell surface expression of DR5 possibly contributes to the enhancement of TRAIL-induced apoptosis.

In a previous study, various small molecule compounds, such as tunicamycin,[14] were reported to transactivate the DR5 gene by the upregulation of CHOP. The inostamycin-induced increase in DR5 mRNA was suppressed in CHOP-knockdown HCT116 cells; however, DR5 protein expression was not suppressed. Furthermore, knockdown of CHOP by siCHOP suppressed only inostamycin-increased CHOP-dependent DR5 mRNA expression, but constitutively expressed DR5 mRNA levels were not affected (Figure 3d). Therefore, in siCHOP-transfected HCT116 cells, inostamycin is considered to increase the protein levels of DR5 translated from constitutively expressed DR5 mRNA by posttranslational modulation. Various studies have reported the mechanism of the transcriptional activation of DR5 gene. However, little is known about the mechanism of translation, posttranslational modification, localization or degradation of DR5. Because of the data presented in this study, inostamycin may be a good bioprobe for use in investigating the regulatory mechanism of DR5 protein. Furthermore, elucidation of the mechanism by which inostamycin increases the expression of DR5 on the cell surface may provide a new molecular target for inducing DR5 upregulation to overcome TRAIL resistance.

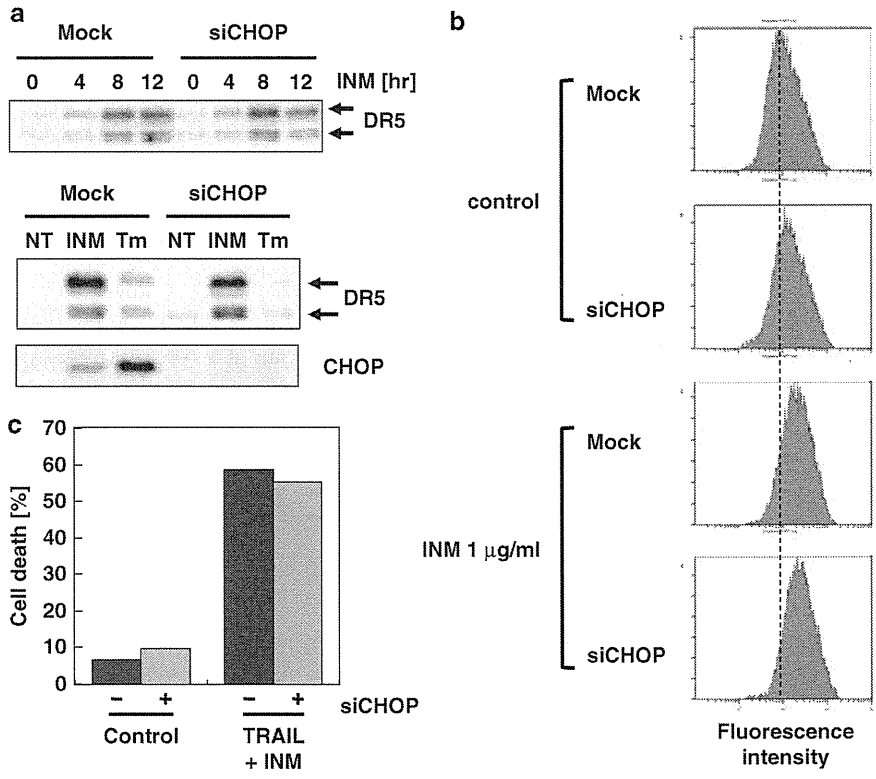

Figure 4 Inostamycin (INM) enhanced tumor necrosis factor-related apoptosis-inducing ligand (TRAIL)-induced apoptosis possibly through CHOP-independent cell surface DR5 upregulation. (**a**) Knockdown of CHOP suppressed tunicamycin (Tm)-induced DR5 upregulation but did not suppress INM-induced DR5 upregulation at protein levels. HCT116 cells were transiently transfected with 20 nM siCHOP. After incubation for 24 h, the transfected cells were treated with 1 $\mu g ml^{-1}$ of INM for 4, 8, 12 h or 10 $\mu g ml^{-1}$ of Tm for 12 h. Cell extracts were prepared for western blotting to detect the expression of DR5. (**b**) Knockdown of CHOP did not suppress the INM-induced upregulation of cell surface DR5. HCT116 cells were transiently transfected with 20 nM siCHOP. After incubation for 24 h, the transfected cells were treated with 1 $\mu g ml^{-1}$ of INM for 12 h. The cell surface DR5 was stained with PE-conjugated DR5 antibody and then detected using a flow cytometer. (**c**) Knockdown of CHOP did not suppress the induction of apoptosis by co-treatment with INM and TRAIL. HCT116 cells were transiently transfected with 20 nM siCHOP. After incubation for 24 h, the transfected cells were treated with or without 1 $\mu g ml^{-1}$ INM together with 10 $ng ml^{-1}$ TRAIL for 18 h. The cells were stained with propidium iodide (PI), and sub-G_1 phase cells were detected using a flow cytometer.

ACKNOWLEDGEMENTS

This work was supported by a Grant-in-Aid for Scientific Research from the Ministry of Education, Culture, Sports, Science and Technology of Japan. This study was partially supported by the Global COE program for Human Metabolomic Systems Biology from MEXT, Japan.

1 Wiley, S. R. *et al.* Identification and characterization of a new member of the TNF family that induces apoptosis. *Immunity* **3,** 673–682 (1995).
2 Pitti, R. M. *et al.* Induction of apoptosis by Apo-2 ligand, a new member of the tumor necrosis factor cytokine family. *J. Biol. Chem.* **271,** 12687–12690 (1996).
3 Ashkenazi, A. & Dixit, V. M. Death receptors: signaling and modulation. *Science* **281,** 1305–1308 (1998).
4 Zhang, X. D. *et al.* Relation of TNF-related apoptosis-inducing ligand (TRAIL) receptor and FLICE-inhibitory protein expression to TRAIL-induced apoptosis of melanoma. *Cancer Res.* **59,** 2747–2753 (1999).
5 Walczak, H. *et al.* Tumoricidal activity of tumor necrosis factor-related apoptosis-inducing ligand *in vivo*. *Nat. Med.* **5,** 157–163 (1999).
6 Pan, G. *et al.* The receptor for the cytotoxic ligand TRAIL. *Science* **276,** 111–113 (1997).
7 Pan, G. *et al.* An antagonist decoy receptor and a death domain-containing receptor for TRAIL. *Science* **277,** 815–818 (1997).
8 Ashkenazi, A. & Dixit, V. M. Apoptosis control by death and decoy receptors. *Curr. Opin. Cell. Biol.* **11,** 255–260 (1999).
9 Sheridan, J. P. *et al.* Control of TRAIL-induced apoptosis by a family of signaling and decoy receptors. *Science* **277,** 818–821 (1997).
10 Nagane, M. *et al.* Increased death receptor 5 expression by chemotherapeutic agents in human gliomas causes synergistic cytotoxicity with tumor necrosis factor-related apoptosis-inducing ligand *in vitro* and *in vivo*. *Cancer Res.* **60,** 847–853 (2000).
11 Wu, G. S. *et al.* KILLER/DR5 is a DNA damage-inducible p53-regulated death receptor gene. *Nat. Genet.* **17,** 141–143 (1997).
12 Sheikh, M. S. *et al.* p53-dependent and -independent regulation of the death receptor KILLER/DR5 gene expression in response to genotoxic stress and tumor necrosis factor alpha. *Cancer Res.* **58,** 1593–1598 (1998).
13 Liu, X. *et al.* The proteasome inhibitor PS-341 (bortezomib) up-regulates DR5 expression leading to induction of apoptosis and enhancement of TRAIL-induced apoptosis despite up-regulation of c-FLIP and survivin expression in human NSCLC cells. *Cancer Res.* **67,** 4981–4988 (2007).
14 Shiraishi, T. *et al.* Tunicamycin enhances tumor necrosis factor-related apoptosis-inducing ligand-induced apoptosis in human prostate cancer cells. *Cancer Res.* **65,** 6364–6370 (2005).
15 Lim, J. H., Park, J. W., Choi, K. S., Park, Y. B. & Kwon, T. K. Rottlerin induces apoptosis via death receptor 5 (DR5) upregulation through CHOP-dependent and PKC delta-independent mechanism in human malignant tumor cells. *Carcinogenesis* **30,** 729–736 (2009).
16 Kikuchi, H. *et al.* Brandisianins A-F, isoflavonoids isolated from Millettia brandisiana in a screening program for death-receptor expression enhancement activity. *J. Nat. Prod.* **70,** 1910–1914 (2007).
17 Son, Y. G. *et al.* Silibinin sensitizes human glioma cells to TRAIL-mediated apoptosis via DR5 up-regulation and down-regulation of c-FLIP and survivin. *Cancer Res.* **67,** 8274–8284 (2007).
18 Kim, Y. H., Park, J. W., Lee, J. Y. & Kwon, T. K. Sodium butyrate sensitizes TRAIL-mediated apoptosis by induction of transcription from the DR5 gene promoter through Sp1 sites in colon cancer cells. *Carcinogenesis* **25,** 1813–1820 (2004).
19 Imoto, M. *et al.* Isolation and structure determination of inostamycin, a novel inhibitor of phosphatidylinositol turnover. *J. Nat. Prod.* **53,** 825–829 (1990).
20 Walczak, H. *et al.* TRAIL-R2: a novel apoptosis-mediating receptor for TRAIL. *Embo. J.* **16,** 5386–5397 (1997).
21 Screaton, G. R. *et al.* TRICK2, a new alternatively spliced receptor that transduces the cytotoxic signal from TRAIL. *Curr. Biol.* **7,** 693–696 (1997).
22 Yoshida, T. *et al.* Proteasome inhibitor MG132 induces death receptor 5 through CCAAT/enhancer-binding protein homologous protein. *Cancer Res.* **65,** 5662–5667 (2005).

ACS chemical biology

Articles

pubs.acs.org/acschemicalbiology

Xanthohumol Impairs Autophagosome Maturation through Direct Inhibition of Valosin-Containing Protein

Yukiko Sasazawa,[†,#] Shuhei Kanagaki,[†,#] Etsu Tashiro,[†] Toshihiko Nogawa,[‡] Makoto Muroi,[‡] Yasumitsu Kondoh,[‡] Hiroyuki Osada,[‡] and Masaya Imoto*[,†]

[†]Faculty of Science and Technology, Department of Biosciences and Informatics, Keio University, Yokohama 223-8522, Japan

[‡]Chemical Biology Core Facility, Chemical Biology Department, RIKEN Advanced Science Institute, Saitama 351-0198, Japan

ABSTRACT: Autophagy is a bulk, nonspecific protein degradation pathway that is involved in the pathogenesis of cancer and neurodegenerative disease. Here, we observed that xanthohumol (XN), a prenylated chalcone present in hops (*Humulus lupulus* L.) and beer, modulates autophagy. By using XN-immobilized beads, valosin-containing protein (VCP) was identified as a XN-binding protein. VCP has been reported to be an essential protein for autophagosome maturation. Using an *in vitro* pull down assay, we showed that XN bound directly to the N domain, which is known to mediate cofactor and substrate binding to VCP. These data indicated that XN inhibited the function of VCP, thereby allowing the impairment of autophagosome maturation and resulting in the accumulation of microtubule-associated protein 1 light chain 3-II (LC3-II). This is the first report demonstrating XN as a VCP inhibitor that binds directly to the N domain of VCP. Our finding that XN bound to and inactivated VCP not only reveals the molecular mechanism of XN-modulated autophagy but may also explain how XN exhibits various biological activities that have been reported previously.

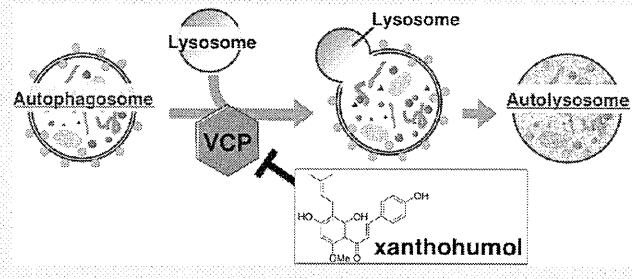

Macroautophagy (herein referred to as autophagy) is an evolutionarily conserved pathway for degradation of intracellular components including organelles, which is critical for the maintenance of cellular homeostasis. Initially, the cytoplasmic components are sequestered by a unique membrane, referred to as an isolation membrane. Dynamic membrane organization is activated from small membrane particles to autophagosomes by the recruitment of autophagy related genes (ATGs) and microtubule-associated 1 light chain 3 (LC3).[1]

The next stage involves the fusion of autophagosomes with lysosomes and subsequent formation of autolysosomes. The inner membrane of the autophagosomes and the cytoplasm-derived materials contained in the autophagosomes are then degraded by lysosomal hydrolases.[2] The amino acids, which are produced by protein degradation, are then returned to the cytoplasm by lysosomal membrane permeases for reuse. Autophagy occurs in all cells at low basal levels under normal conditions to maintain homeostasis. It has been reported that aberrance of autophagy is involved in the pathogenesis of many diseases including neurodegenerative disease,[3,4] cancer,[5] muscle atrophy, and type 2 diabetes.[6]

Despite identification of more than 30 ATGs,[7,8] the molecular mechanism of autophagy is still not fully understood. Studying autophagy through chemical genetics could be an ideal approach to gaining a better understanding of autophagy signaling pathways. Most compounds that have been reported to be regulators of autophagy are distributed between two major groups. One group induces autophagy by inhibiting PI3K/Akt/mTOR signaling,[9] which is the major inhibitory signal that suppresses autophagy. The other group of regulators suppresses autophagy by inhibiting class III PI3K,[10] which is the homologue of yeast VPS34 and is required for the onset of autophagy.

In this study, we explored the mechanism of autophagy and identified additional small compounds that could modulate this process. This was done by screening for a small compound from an in-house natural product library using EGFP-LC3 stably expressing HeLa cells, and we identified xanthohumol (XN) as an autophagy modulator. Xanthohumol (30-[3,3-dimethyl allyl]-20,40,4-trihydroxy-60-methoxychalcone) is the principal prenylated chalcone of the female inflorescences of the hop plant ("hops"), an ingredient of beer.[11] Human exposure to XN is primarily through beer consumption. Several studies have reported on the potential health benefits of XN, including inhibition of diacylglycerol acyltransferase,[12,13] apoptosis induction,[14] NF-kappa B inhibition,[15] and ER stress induction.[16] However, there are no reports that show the relevance of XN to autophagy. Thus, to understand the mechanism by which XN modulates autophagy, we attempted to identify the target protein of XN responsible for the regulation of autophagy.

Received: November 28, 2011
Accepted: February 23, 2012

   dx.doi.org/10.1021/cb200492h | *ACS Chem. Biol.* XXXX, XXX, XXX–XXX